2011

Determination of a new throttling liquid rocket engine for a Mars lander

Erin M. Betts

DETERMINATION OF A NEW THROTTLING LIQUID ROCKET ENGINE FOR A MARS LANDER

by

ERIN M. BETTS

A THESIS

Submitted in partial fulfillment of the requirements
for the degree of Master of Science in Engineering
in
The Department of Mechanical and Aerospace Engineering
to
The School of Graduate Studies
of
The University of Alabama in Huntsville

HUNTSVILLE, ALABAMA
2011

In presenting this thesis in partial fulfillment of the requirements for a master's degree from The University of Alabama in Huntsville, I agree that the Library of this University shall make it freely available for inspection. I further agree that permission for extensive copying for scholarly purposes may be granted by my advisor or, in his/her absence, by the Chair of the Department or the Dean of the School of Graduate Studies. It is also understood that due recognition shall be given to me and to The University of Alabama in Huntsville in any scholarly use which may be made of any material in this thesis.

Erin M. Botta 4/13/2011

(student signature) (date)

THESIS APPROVAL FORM

Submitted by Erin M. Betts in partial fulfillment of the requirements for the degree of Master of Science in Engineering in Mechanical Engineering and accepted on behalf of the Faculty of the School of Graduate Studies by the thesis committee.

We, the undersigned members of the Graduate Faculty of The University of Alabama in Huntsville, certify that we have advised and/or supervised the candidate on the work described in this thesis. We further certify that we have reviewed the thesis manuscript and approve it in partial fulfillment of the requirements for the degree of Master of Science in Engineering in Mechanical Engineering.

Robert A Frederick 3/9/11
Committee Chair
(Date)

3/8/11
Committee Member
(Date)

3/8/11
Committee Member
(Date)

Robert A Frederick Jr 3/9/11
Department Chair
(Date)

03/09/11
College Dean
(Date)

Rhonda Kay Gaede 4/18/11
Graduate Dean
(Date)

ABSTRACT

The School of Graduate Studies
The University of Alabama in Huntsville

Degree: Master of Science in Engineering College/Dept: Engineering/Mechanical and Aerospace Engineering

Name of Candidate: Erin Mae Betts
Title: Determination of a New Throttling Liquid Rocket Engine for a Mars Lander

As NASA begins a new era of space exploration, it is recognized that a series of rocket engines will be required in order to complete object and planetary landing missions. NASA preliminary studies have indicated that a 15,000 lbf thrust LOX-methane engine with 10:1 throttling capability is a desired propulsion configuration for a Mars lander. The objective of this study is to validate a workable LOX-methane engine that is capable of a 10:1 throttling ratio for such an application. The new Mars landing engine designed herein uses components that are desired to successfully throttle the engine. A power balance model is developed, and it is determined that using an expander cycle engine with LOX-methane propellants, a pintle injector, independently driven LOX and methane turbopumps, with a thrust control valve and oxidizer control valve is a viable option for a throttleable Mars landing engine. The engine operates at a chamber pressure of 800 psia at 100% power and 80 psia at 10% power and a mixture ratio of 3.3 at both power levels. The injector is capable of achieving a ratio of $\Delta p/p_c$ of 20% at all power levels. The oxidizer and fuel turbopumps generate 58.87 Hp and 170 Hp at 100% power, and 2.67 Hp and 25 Hp at 10% power respectively.

Abstract Approval: Committee Chair Robert A Frederick

Department Chair Robert A Frederick

Graduate Dean Rhonda Kay Gaede

ACKNOWLEDGMENTS

I would like to thank Dr. Robert A. Frederick for his advising and encouragement throughout the development of this thesis. His support and guidance is greatly appreciated. I would also like to thank Dr. D. Brian Landrum and Dr. David Lineberry for being on my thesis committee and for helping and advising me along this journey.

I would also like to thank Joseph Leahy at NASA Marshall Space Flight Center for his guidance and advice during all phases of the progression of this paper. His expertise and willingness to share from his years of experience is truly valued. Jason Turpin and Huy Hien Nguyen were also very helpful as mentors and as systems engineers; they helped greatly in providing help with evaluating the throttling engine as a system. The time spent advising and guiding is greatly appreciated.

I would also like to thank Matthew Casiano for his help in finding resources and discussing throttling methods in detail; Erika Alvarez and Matthew Marsh for their guidance in the turbomachinery area; Joseph Ruf and Paul Gradl for their expertise on nozzle design and flow separation; and Gregg Jones for his expertise on injector design. Everyone named above works at the NASA Marshall Space Flight Center in the Propulsion Engineering Directorate.

Much of what was learned during this study cannot be found in textbooks; it's the people who have the experience and are willing to share their experiences that have allowed me to truly grow as an engineer during the writing of this thesis.

I also owe a great deal of appreciation to my husband, Jason Betts, for supporting me and encouraging me throughout this study.

TABLE OF CONTENTS

LIST OF FIGURES

LIST OF TABLES

LIST OF ABBREVIATIONS AND/OR ACRONYMS

AIAA	American Institute of Aeronautics and Astronautics
Btu	British Thermal Unit
CEA	Chemical Equilibrium with Applications
CECE	Common Extensible Cryogenic Engine
CEQUEL	Chemical Equilibrium in Excel
c_f	Thrust Coefficient
Δp	Pressure Drop
FSS	Free Shock Separation
ft^3	Cubic Foot
FTBV	Fuel Turbine Bypass Valve
gpm	Gallons per Minute
Hp	Horsepower
in^2	Square Inch
I_{sp}	Specific Impulse
lbf	pound-force
lbm	Pound-mass
LH_2	Liquid Hydrogen
LLDET	Lunar Lander Descent Engine Testbed
LMDE	Lunar Module Descent Engine
LOX or LO_2	Liquid Oxygen
MOV	Main Oxidizer Valve
MFV	Main Fuel Valve
MSFC	Marshall Space Flight Center
MTBV	Main Turbine Bypass Valve
N	Speed
N_2H_4	Hydrazine
N_2O_4	Nitrogen Tetroxide
NASA	National Aeronautics and Space Administration

OCV	Oxidizer Control Valve
p_c	Chamber Pressure
PL	Power Level
psia	pounds -force per square inch absolute
Q	Volumetric Flowrate
R	Rankine
RAD	Rocket-Assisted Descent
RSS	Restricted Shock Sepataion
s	Second
SSME	Space Shuttle Main Engine
TBV	Turbine Bypass Valve
TCV	Thrust Control Valve
UDMH	Unsymmetrical Dimethylhydrazine

CHAPTER ONE

INTRODUCTION

As the National Aeronautics and Space Administration (NASA) begins a new era of space exploration, it is recognized that a series of rocket engines will be required in order to complete object and planetary landing missions. In particular, it is expected that NASA will land humans on Mars in the 21st century. In order to land on Mars, vehicle deceleration using a throttleable liquid rocket engine is desirable in order to have control over the landing phase of the mission.

This study takes the requirements for a Mars landing engine into consideration in designing a new and innovative throttling liquid rocket engine. The engine has a thrust range of 15,000 to 1,500 lbf, a pintle injector, a regenerative cooled thrust chamber, and independently driven liquid oxygen (LOX) and methane turbopumps. The propellants LOX and methane are chosen due to the ability to mine the propellants "in-situ" from the Martian surface for the return mission. Methane is also a good propellant choice for the out-bound mission since it has a high density that allows for more compact tanks than those required for hydrogen, high specific impulse, good coolant properties, and the ability to be stored as a liquid during the in-space journey. One downside to using methane, however, is the lack of performance data available. As many engines in the

United States have traditionally used LOX and hydrogen or LOX and kerosene, the throttled performance of an engine using methane is not well characterized.

Designing a throttleable engine is challenging. The key difficulty in throttling liquid rocket engines is maintaining an adequate pressure drop across the injector, which is necessary to provide propellant atomization and mixing.[1] In addition to maintaining good combustion in the combustion chamber, is it critical to evaluate the key rocket engine components such as the thrust chamber, turbomachinery, valves, and nozzle to ensure each component is adequately designed for the range of thrust that is required of the engine. For the combustion chamber, cooling can be an issue at low thrust levels. For turbomachinery, the primary considerations are to avoid cavitation, stall, surge, and to consider bearing leakage flows, rotordynamics, and structural dynamics. For valves, it is necessary to design valves and actuators that can achieve accurate flow control at all thrust levels. For the nozzle, it is important to assess the amount of flow separation that can be tolerated at low thrust levels for ground testing.

This study begins by discussing throttling and how engines are able to throttle. Two key engines that have successfully demonstrated throttling are evaluated, followed by a breakdown of components in order to discuss special considerations that need to be made for engine throttling. After this engine system assessment is made, the author draws conclusions on a new and innovative configuration that could be used to build a new throttling liquid rocket engine based on initial requirements for a Mars lander. A power balance model is built to perform a top-level steady state analysis of a new engine design that is capable of operating at 15,000 lbf and 1,500 lbf thrust. Figure 1.1 outlines the overall process flow for this design study.

The conclusion from this study is that a new Mars landing engine could feasibly consist of LOX-methane propellants, an expander cycle, independently driven fuel and oxidizer turbopumps, and a pintle injector. An engine balance model is designed, and the steady state performance of each component is determined. The performance of the components fall within reasonable expectations based on comparison to similar rocket engines. However, due to the use of methane as a propellant, there is little data available to compare the methane pump and coolant performance to. Obtaining adequate heat flux in the regenerative coolant section of the engine proves to be critical for success of the expander cycle engine configuration. The engine operates at a chamber pressure of 800 psia at 100% power and 80 psia at 10% power and a mixture ratio of 3.3 at both power levels. The injector is capable of achieving a ratio of $\Delta p/p_c$ of 20% at all power levels. The oxidizer and fuel turbopumps generate 58.87 Hp and 170 Hp at 100% power, and 2.67 Hp and 25 Hp at 10% power respectively.

The model developed in this study is validated to the extent that the calculations for component performance are checked against results obtained for J-2X and RL-10. Where evaluated, there is good agreement between results obtained using this model and results obtained by the governing models for these engines.

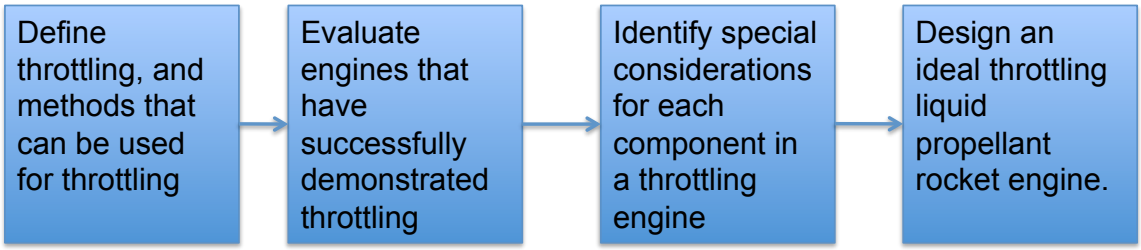

Figure 1.1: Overall Process Flow for Design Study

CHAPTER TWO

BACKGROUND

2.1 Throttling Equations

In order to begin the discussion on throttling liquid rocket engines, it is first necessary to understand the basic thrust equation. The thrust equation contains both a momentum exchange term and pressure balance term to describe overall engine thrust,

$$F = \dot{m}v_e + (p_e - p_a)A_e \quad (2.1)$$

In this equation, F is thrust, m is mass flow rate through the nozzle, v_e is the velocity of the hot gas at the exit of the nozzle, p_e is the pressure at the exit of the nozzle, p_a is the pressure of the atmosphere immediately outside the nozzle, and A_e is the nozzle exit area.

When evaluating this equation, it can be observed that the thrust can be decreased if ambient pressure is increased, or if mass flow rate, exit velocity, exit pressure, or exit area is decreased. Varying the nozzle exit area is difficult to achieve, since high thermal loads would possibly inhibit the mechanical features of a moveable nozzle.[2] Varying the propellant flow rates has been shown to be a favorable way to vary thrust; several methods for varying propellant flow rates in an effort to throttle the engine are discussed throughout this evaluation.

When throttling an engine, the key is to reduce the thrust and chamber pressure of the rocket by reducing the upstream propellant mass flow rates and still maintaining adequate pressure drop over the injector so that combustion stability can be achieved.

From historical and experimental results, the "general rule of thumb" is that the nominal ratio of injector pressure drop to chamber pressure should be around 15-20% in order to achieve and maintain stable combustion.[3] Although this relationship is a good preliminary design goal, it is not a firm requirement, as there have been engines that have operated at a $\Delta p/p_c$ less than 15% while still achieving stable combustion characteristics, while in other cases, engines can exhibit a low frequency combustion instability commonly referred to as chug operating at a $\Delta p/p_c$ higher than 15%.

2.2 Specific Impulse

In terms of specific impulse, I_{sp}, it is understood that

$$I_{SP} = \frac{F}{\dot{m}g} \quad . \qquad (2.2)$$

At lower thrust levels, the I_{sp} decreases. While the mass flow rate decreases as thrust decreases, the thrust decreases at a greater rate, resulting in a loss of I_{sp} as the engine is throttled. Another way to express I_{sp} is

$$I_{sp} = \frac{c^* c_f}{g} \quad , \qquad (2.3)$$

where c_f is the thrust coefficient, and is a function of the ratio of specific heats, chamber pressure, ambient pressure, and expansion ratio. It reflects the product-gas expansion properties and design quality of the nozzle. As thrust decreases, the expansion quality

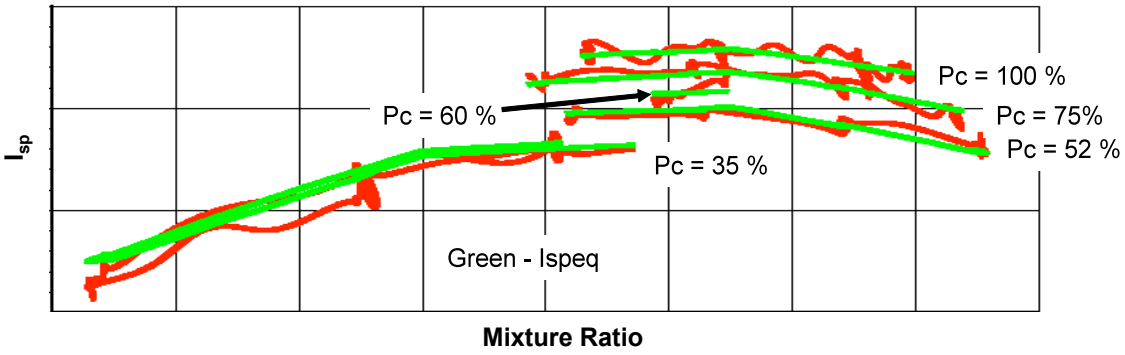

Figure 2.1: CECE I_{sp} vs. Thrust[4]

decreases, and the thrust coefficient decreases. As a result, the I_{sp} decreases at lower thrust levels.

Mixture ratio also plays a role in the specific impulse of the engine. For each engine, there exists an optimum mixture ratio where deviations from the optimum result in lower I_{sp}. This optimum mixture ratio is affected by stay time of the burning gas in the combustion chamber, cooling considerations, and propellant density.[5]

An example of this effect is shown in Figure 2-1, which is a plot of the Common Extensible Cryogenic Engine (CECE) test data. There exists a mixture ratio for optimal I_{sp} at each thrust level. At all mixture ratios, as the thrust level is decreased, the I_{sp} decreases.

2.3 Approaches to Throttling

Once the physics and the equations for throttling are understood, it is useful to understand demonstrated approaches to liquid rocket engine throttling. Gordon Dressler[6] and Matthew Casiano[3] have both written American Institute of Aeronautics and Astronautics (AIAA) papers that address throttling approaches. Combining the ideas in these two papers, liquid propellant rocket engine throttling methods are presented below.

It is important to note that for shallow throttling, one method alone may be employed for throttling. However, as deeper throttling requirements are imposed on a system, several throttling solutions are typically used together. In particular, some additional throttling mechanisms, such as inert gas injection, can be turned on for use when needed at low power levels if the engine can otherwise achieve its objectives without the additional system at higher thrust levels. It is common for the cost of an engine to increase substantially as deeper throttling requirements are imposed due to added mechanical and system design complexity and testing that are required to achieve the mission goals. There are six identified methods for liquid rocket engine throttling.

2.3.1 Using a High-Pressure-Drop Injection System with Propellant Flow Regulation

One way to achieve an adequate pressure ratio at both low and high power levels is to design the injector to have a high-pressure drop at the full power level. Using a high-pressure drop injector for full thrust allows for enough pressure drop to be maintained at low power levels. One issue with this method is that at full thrust, sometimes unreasonably high pressure requirements are imposed on the feed system or the engine is forced to operate at a lower chamber pressure than desired. Due to the limitations that exist with using a high-pressure drop injector, applications are commonly limited to shallow throttling engines such as the Space Shuttle Main Engine (SSME) and RD-180. As the throttle range increases, it is desirable to start with a high-pressure drop injector, but additional system modifications are likely to be required.

One advantage of using a high-pressure drop injector is its operational simplicity. Although multi-element injectors can be difficult to manufacture and require tight tolerances on very small geometries, one injector is required for each engine, and it requires little to no maintenance once it is installed. The absence of mechanically actuated devices and control systems for the injector allows for simple operation; however, if a high-pressure drop injector is coupled with additional dynamic throttling aids, the complexity of the system can increase.

2.3.2 Varying the Injection Element Area by the use of Selectable Manifolds or Movable Injector Elements.

This method uses injector area variation to achieve engine throttling. By varying the flow area of the injected fluids, it is feasible to achieve the desired flow velocities in the combustion chamber while maintaining adequate pressure drop at all thrust levels. This allows for optimized injection at all power levels without having to impose stringent requirements on the feed system or reducing chamber pressure.[3]

A dual or multiple stage injector consists of two or more injector stages that are in series with one another. At low power levels, valves can be used to stop flow to one of the injector stages, thus limiting the propellant flow to a single injector stage. This allows for better optimization of the injection system at both high and low power levels in order to keep the feed system requirements and combustion stability in check. The Lunar Lander Descent Engine Testbed (LLDET) at the Marshall Space Flight Center (MSFC) is currently testing two different dual stage injector designs to evaluate the performance

characteristics in an effort to develop the technology necessary for a new Lunar Lander Descent Engine.[7]

When considering dual or multiple stage injectors, it is clear that a step change occurs when one injector is turned off. It is important to understand the system affects when the injector is turned off, since this action could induce combustion instability and large heat fluxes in a marginally stable system. Complicated purging must be incorporated for the non-operating stage orifices in order to prevent backflow of propellant and combustion gases.[6]

Pintle injection is another form of variable injection area throttling. The pintle injector is mechanically actuated to achieve the proper flow area and stable injection characteristics at all power levels. A Pintle injector was used on the Apollo Lunar Module Descent Engine (LMDE),[8] and although it requires mechanical actuation, the pintle can be a simple component to manufacture. One key characteristic of the pintle is its inherent combustion stability at all power levels.[9]

2.3.3 Inert Gas Injection to Decrease Fluid Density Injected into the System

Inert gas injection injects an inert gas directly upstream of the LOX manifold in the LOX dome. As the gas is injected into the system, the density of the LOX is decreased significantly, which raises the pressure drop over the injector. With gas injection, the pressure drop is increased without affecting the mass flow rate. The volume void fraction of the gas and liquid mixture could increase significantly by increasing the gas mass flow rate by a relatively small amount, while the gas quality (or mass of the gas relative to the total mass) would remain very small.[10] This is a proven way to keep the pressure ratio

high even at low thrust, thus eliminating chug. However, caution must be used when employing this method, since "Russian experience reports that gas injection can lead to the onset of high frequency pressure fluctuations."[3]

Disadvantages to this method are that it requires additional complexity in the feed system, and system compliance can be impacted, which can lead to instabilities other than chug. Also, inert gas can be quite expensive, so using large amounts is not always economical.

2.3.4 Use of Multiple Combustion Chambers

Using a single feed system, two or more combustion chambers can be used to achieve the desired thrust. Chambers can be turned on or off in order to control overall thrust, or each chamber can be optimized to a smaller throttle ratio in order to achieve a net throttling affect. The RD-180 uses multiple chambers to meet the durability and high performance requirements of the Atlas vehicle.[11] For engines such as the RD-180 that are driven by a single set of turbomachinery, many of the system effects that are present in the single chamber configuration are still present using multiple chambers. Some issues that can arise from this throttling method include a changing thrust reaction point on the vehicle and added system complexity and weight. The use of multiple chambers, however, allows for a decrease in engine length, which is desirable for some missions.

2.3.5 Varying Nozzle Throat Area

Varying the throat area is a technique that can be used to vary thrust; this method is called "throat throttling." This can be achieved by mechanically restricting the throat area

or by using a gas to vary the throat area. “Both methods effectively changed the throat area by providing some blockage into the flow field. Both modes have a net effect on decreasing thrust, since at constant propellant pressures, a throat restriction causes an increase in chamber pressure and hence lower injection pressure drops and reduced propellant flow rates.”[3]

This is more likely an option for smaller thrusters rather than large boost engines due to the mechanical difficulties and high heat fluxes and structural loading that the throat experiences during engine operation. Also, large changes in throat area are required in order to affect small changes in thrust.[6]

2.4 Alternate Approaches to Throttling

Due to difficulties with liquid rocket engine throttling, it is typical that design teams will attempt to think of ways to avoid throttling. Alternate methods that have been used in the past include pulse modulation, using multiple engines, and vehicle design.

2.4.1 Pulse Modulation

Pulsing is typically acceptable for use on low thrust or monopropellant engines, where valves and short impulses can be used to achieve a desired total impulse or average thrust. Pulsing is common in attitude control and some landing configurations. It can also be useful for rendezvous applications where small adjustments in position are desired. Some examples of pulsing engines include engines that descend from the LMDE,[12] and roll control systems that are commonly used on launch vehicles. Hypergolic propellants are good choices for propellants for pulsing engines since they do not require an ignition

source for each impulse. Pulse modulation has been effective in military applications for thrust vector control and for interceptors.[13]

Some disadvantages to this method include transients and shock loading on the vehicle structure, heat soak-back into the combustion chamber head-end, and inefficient propellant use due to chamber cooling and dribble losses between pulses. Also, engines typically are most efficient at steady state and least efficient during start-up and shut-down transients. Thus, pulsing tends to be somewhat inefficient from a propellant usage standpoint due to the frequency of transient phase operation.[6]

2.4.2 Multiple Engines

Multiple engines can be used so that certain engines can be turned on or off to control the thrust. Multiple engine configurations have been proposed for lunar and planetary landers. One issues with using multiple engines is in controlling the vehicle with a changing center of gravity as certain engines are turned on and off. Engines would also have to have relight capabilities, which could lead to increases in test time and thus higher development costs. Using multiple engines also introduces system complexity, but can increase total system reliability since one or more engines could fail without resulting in loss of the mission.

2.4.3 Vehicle Design[14]

Vehicle design can be creative in order to avoid throttling entirely, or to keep throttling to a reasonable, shallow range. For lunar landing missions, several ideas have been presented to avoid the complexities of throttling. One idea is that a two-stage thrust axis

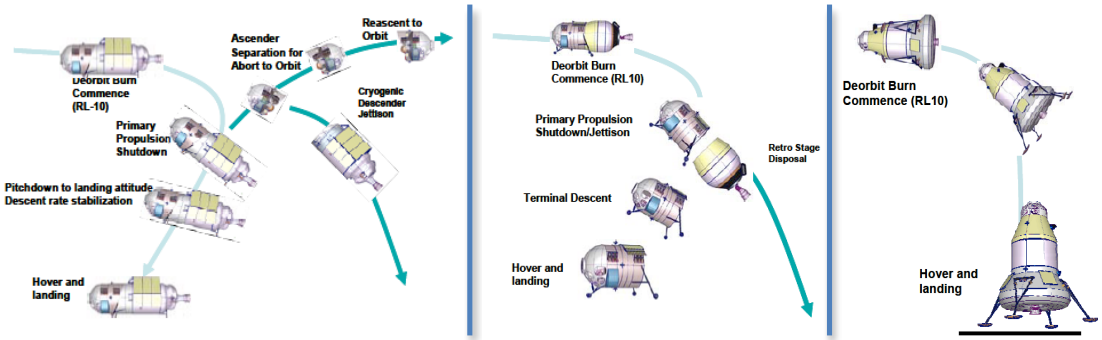

Figure 2.2: Vehicle Design Solutions for Lunar Lander[14]

lander could be used for lunar landing; an RL-10 engine could be used for the primary descent, and the vehicle could rotate on its side and use smaller thrusters for a soft landing. Another idea is that the system could jettison the descent propulsion system shortly before landing. A third idea is that a single stage propulsion system could be used for both lunar descent and ascent. This could incorporate weight savings and could utilize in-situ resources from the moon for fuel. These basic concepts are shown in Figure 2.2.

Another technique was successfully used for the Mars lander that safely carried the Spirit and Opportunity rovers to the Martian surface. Parachutes were used for the initial approach, followed by the deployment of 24 Vectran airbags to soften the landing. Three Rocket-Assisted Descent (RAD) motors were developed to assist, if necessary, in the final landing phase. This landing system achieved deceleration from 12,000 miles per hour down to about 12 miles per hour. The airbags were specially designed to withstand the impact and protruding geological features on the Martian surface.[15]

2.5 Throttleable Engines

Despite the difficulties associated with throttling, it has been successfully achieved on numerous liquid rocket engines.[16] This study focuses on two engines in particular, the

LMDE and the RL-10 and derivatives, which have different cycles, applications, propellants, and component design. These engines are studied since they are close to the size of interest for a Mars landing engine, and they both have successfully demonstrated a high range of throttleability. By understanding how these two engines have been successful, it is believed that the best features from each engine can be used to design an "optimal" throttling engine.

2.5.1 Lunar Module Descent Engine

The development of the Lunar Module Descent Engine began in 1963 at TRW Systems in support of the Apollo missions to the moon. The LMDE was instrumental in the lunar landings of Apollo 11, 12, 14, 15, 16, and 17. It also returned the astronauts to Earth after the service module failure on Apollo 13.[17]

Some of the key requirements for the LMDE include accurate thrust and mixture ratio

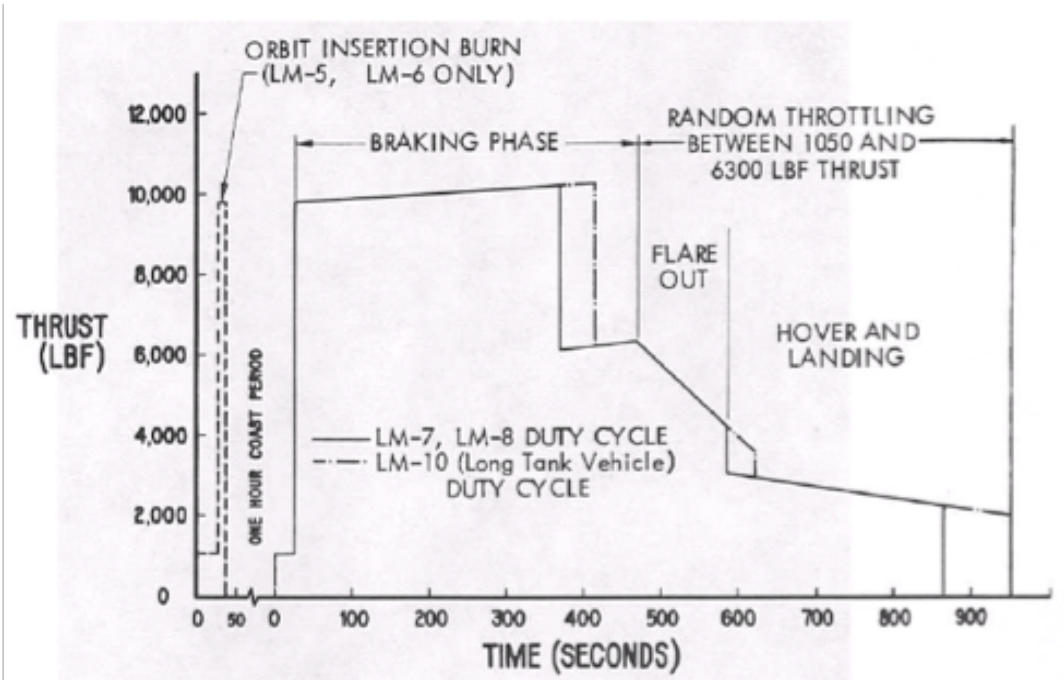

Figure 2.3: LMDE Nominal Duty Cycle[6]

control, accurate propellant injection control to maintain optimum performance and combustion stability, ability to perform multiple, space-vacuum restarts at 10% or higher throttle level without startup ignition spikes and without hydraulic instabilities, and high reliability.[9]

The LMDE is a pressure-fed engine that uses the earth-storable hypergolic bipropellants nitrogen tetroxide (N_2O_4) and Aerozine 50/50 (N_2H_4/UDMH). The LMDE achieves a maximum thrust of 10,000 lbf with a vacuum I_{sp} of about 305 seconds at maximum thrust. The simplicity of the LMDE and the use of hypergolic propellants increases the reliability of the engine, although the hypergolic propellants cannot achieve the high I_{sp} that is achieved using liquid hydrogen and liquid oxygen propellants.

The LMDE is required to perform the thrust profile shown in Figure 2.3, with a throttle ratio of 10:1. This was the first engine to successfully demonstrate 10:1 throttling on a manned space flight mission.

The unique design features of the LMDE allow for this wide performance range. These features include a variable area pintle injector and cavitating venturi flow control valves. The use of these features together isolates the propellant flow control function from the propellant injection function, which allows for optimization of each function without compromising the other. The pintle injector that is used on this engine is discussed in further detail in the Injector section of this paper. The LMDE never experienced sustained high-frequency instability, which is primarily attributed to the inherent stability of the pintle injector design.[9]

2.5.2 RL-10 and Derivatives

The RL-10 development began in 1958 by Pratt & Whitney.[18] The RL-10 has proven to be a very versatile engine, and has survived over five decades to be a proven, highly throttleable and highly reliable engine. The RL-10 has evolved for several different applications, including use as an upper stage on the Titan III, Titan IV, Delta III, Atlas I, Atlas II, Atlas IIA, and Atlas IIAS. It was also used for the DC-X vehicle, and the CECE derivation of the RL-10 was tested through 2010 at Pratt & Whitney Rocketdyne in West Palm Beach, Florida. The CECE is the "RL-10" focus of this study since it is a recent, relevant engine that has successfully demonstrated throttling in excess of 10:1.[4] The maximum thrust of the CECE is about 15,000 lbf.

The RL-10 has demonstrated the ability to operate using a number of different

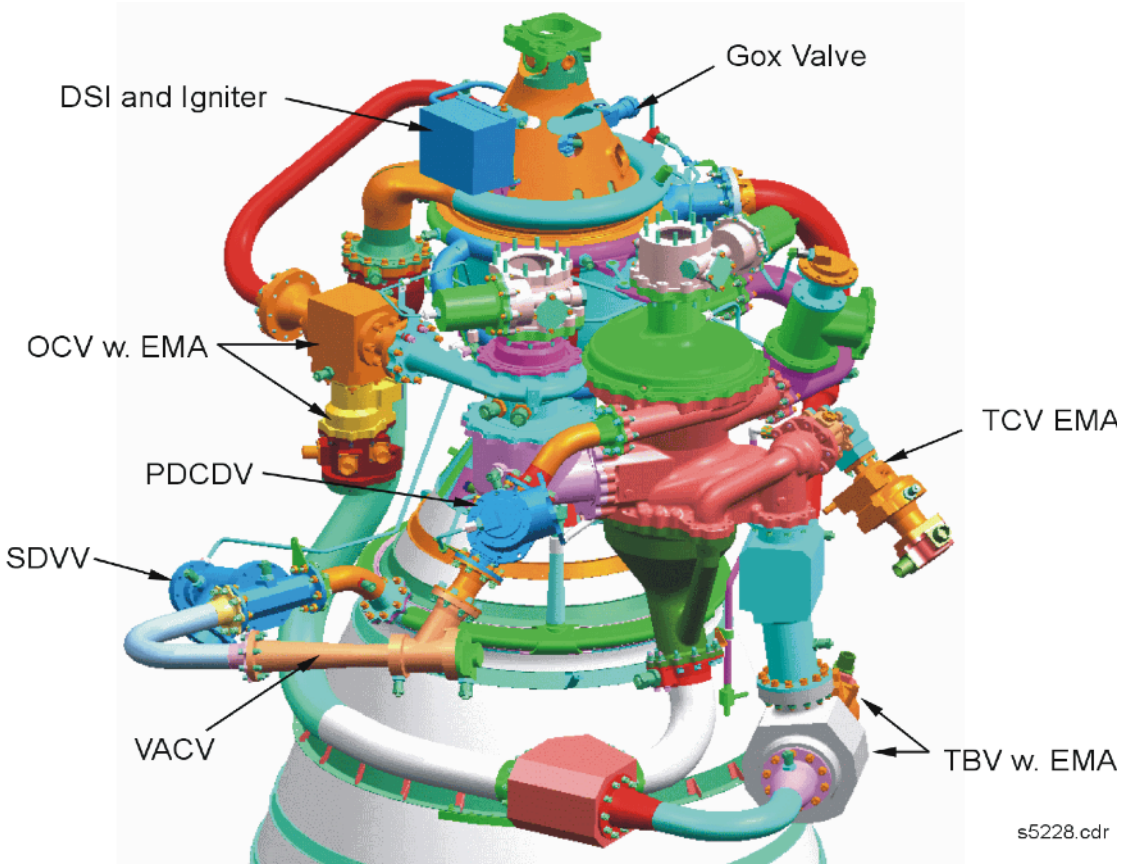

Figure 2.4: RL-10 CECE Unique Valve Configuration[4]

propellant combinations, including Fluorine/Hydrogen, FLOX-methane, and LOX/Propane, in addition to the baseline LOX/Hydrogen. The key requirements that the RL-10 was designed to were low cost, high reliability, and simple control.

The RL-10 uses a closed expander cycle.[19] The fuel pump pumps the cold fuel through the combustion chamber coolant tubes. The gas is heated through the heat transfer process as it flows through the regenerative coolant tubes, and is routed through the turbine to power the turbopump assembly. A single turbine is used with a geared LOX and Hydrogen pump assembly. The expander cycle is quite benign, which is advantageous in particular to the turbine; the low turbine temperatures allow the RL-10 to use lightweight materials to keep engine weight to a minimum. This is in sharp contrast to high temperature turbines that are driven directly by combustion gases, such as those used in the SSME, J-2S, and RD-180.

Key features of the CECE allow the engine to achieve throttling. These are turbine bypass valve (TBV), thrust control valve (TCV), RL-10 venturi, cavitating venturi, and variable oxidizer control valve (OCV). Figure 2.4 shows the CECE unique valve configuration.

2.5.3 Throttling Engine Summary

Table 2.1 summarizes the LMDE and RL10/CECE liquid rocket engines that are studied herein.

Table 2.1: Summary of Two Throttling Liquid Rocket Engines

	LMDE	RL10/CECE
Performance		
Max Vacuum Thrust (lb_f)	10,000	15,000
Vacuum I_{sp} (sec)	305	445
Throttle Ratio	10-to-1 (10% to 100%)	10-to-1 (10% to 100%)
Design Features		
Cycle	Pressure Fed	Closed Expander Cycle
Propellants	N_2O_4 and Aerozine 50/50	LO_2 and LH_2
Turbopumps	None	Geared, driven by fuel turbine
Injector	Pintle	Multi-element injector

CHAPTER THREE

ENGINE SYSTEMS ASSESSMENT

Throttling is an engine systems issue that impacts each component in the liquid rocket engine. The previous section described brief details of two throttleable engines. These two engines are now evaluated with a discussion of the separate engine components, and particular issues that may be encountered with a given component. It is important to evaluate the engine cycle that is used and the component interactions, along with the propellants that are used in order to achieve an understanding of how the system will operate at varied thrust levels. Although predictions are useful in the design phase, it is of the utmost importance to invest in a thorough test program that allows for component and engine system testing to understand the limitations of the hardware.

This focus of this chapter is to identify what may be the desired configuration for each component, as it would function in a throttling engine. Some design features are highly desired in a throttling engine, and the purpose of this chapter is to identify what the desirable features are.

3.1 Injector

The liquid rocket engine injector is one of the most sensitive and complex components of the engine. The purpose of the injector is to inject “the propellants into the combustion

chamber in the right proportions and the right conditions to yield an efficient, stable combustion process."[5] Injector design consists of a fine balance between combustion stability, injector element size and number, combustion efficiency, manufacturing complexity, and cost.

Proper propellant atomization, vaporization, and mixing is the primary design goal of the injector; setting a high enough pressure drop over the injector ensures high propellant velocities to achieve good propellant atomization and mixing once the propellants enter the combustion chamber. Propellant velocities and injection patterns are also optimized for proper combustion.

As discussed previously, a typical "rule of thumb" when designing an injector is to keep the ratio of injector pressure drop to chamber pressure around 15-25%. This is particularly important for LOX injection. While a low pressure drop minimizes the injector weight and requirements on the feed system, the pressure drop needs to be high enough in order to prevent communication between the chamber gases and the feed system, which leads to instabilities. When throttling liquid rocket engines, two primary combustion instabilities issues may arise; chug and LOX boiling.

3.1.1 Chug

One problem that is typical of development throttling engines is a phenomenon called chug. Chug is a low frequency instability that occurs between 10 and 400 Hz. It is commonly driven by communication between propellant combustion in the combustion chamber and fluid dynamics just upstream of the injector in the propellant feed system. Employing adequate pressure drop over the injector can usually eliminate chug.

Additional methods of avoiding chug are using dual element injectors, gas-gas injection, and high inertia injectors.[20] Chugging is particularly a problem at low thrust on the RL-10 CECE.

Chug is also dependent on mixture ratio. Inert gas injection can be turned on at the low thrust levels that are susceptible to chug in order to eliminate the chug. As discussed above, the purpose of gas injection is to increase the pressure drop over the injector by lowering the density of the injected fluid. For a given mass flow rate of propellant, assuming constant C_d and A, when the gas is injected into the LOX cavity, the injected LOX becomes a mixture of LOX and gas, with a density that is considerably lower than LOX alone. Since density and pressure drop are inversely related, as the density decreases, the pressure drop increases. Thus, with gas injection, adequate pressure drops can be achieved at low power levels such that chug can be avoided. This was successfully demonstrated using Helium injection on the RL10.[21]

One disadvantage of gas injection is that the gas has a tendency to "soften" the system by increasing the system's capacitance. This can counteract some of stability benefits of the pressure drop gained by using gas injection. Instabilities can also be caused if the gas is not injected into the system correctly or if the gas is not a clean, homogeneous mixture. If the flow rate of the gas is not sufficient, it may not be effective. While the gas flow rate matters, gas temperature does not have an affect on chug. LOX boiling can also contribute to chug, primarily due to the fact that the LOX boiling increases the system compliance.

3.1.2 LOX Boiling

LOX boiling is a concern that needs to be considered for deep throttling engines. The LOX enters the LOX cavity of the injector, which is often located adjacent to the fuel injector cavity. In expander cycle engines, the LOX can experience boiling. At lower thrust levels, the pressures in the LOX dome are lower than they are at full thrust. If the pressure drops below the LOX critical pressure, LOX boiling can occur. Also, heat transfer from the fuel feed side can increase the likelihood for LOX boiling. Boiling in the LOX dome is highly undesirable since it can lead to combustion instabilities. The feed temperature of the LOX impacts its likelihood for boiling.

One fix that can be incorporated into the design is to insulate the LOX from the fuel in order to prevent heat transfer from the warm fuel to the LOX. Another method for mitigating this concern is to inject an inert gas just upstream of the LOX injection point in an effort to decrease the overall LOX density and in effect raise the pressures in the LOX dome. Inert gas injection is not only beneficial to achieve an adequate pressure drop over the injector, but it also can be useful in preventing LOX boiling and associated instabilities from occurring.

3.1.3 Injector Types

Several different types of injectors can be used in throttleable engines. In this study, the high Δp single stage multi-element injector, pintle injector, and two or multistage injectors are considered.

3.1.3.1 High Delta Pressure Single Stage Multi-Element Injector

The high Δp single stage multi-element injector is a common injector in American engine designs. The SSME, J-2S, RL-10, and RD-180 engines use high-pressure drop single stage multi-element injectors in order to achieve throttling. Using a high Δp injector allows for adequate pressure drop at low power levels so that combustion stability can be achieved. Multi-element injectors consist of a series of LOX posts that are brazed into the injector faceplate. The use of numerous LOX posts allows for adequate atomization, mixing, and vaporization of the propellants upon entering the combustion chamber.

Multi-element injectors typically exhibit good performance and efficiency. However, they are typically limited to use with shallow throttling applications such as boost or

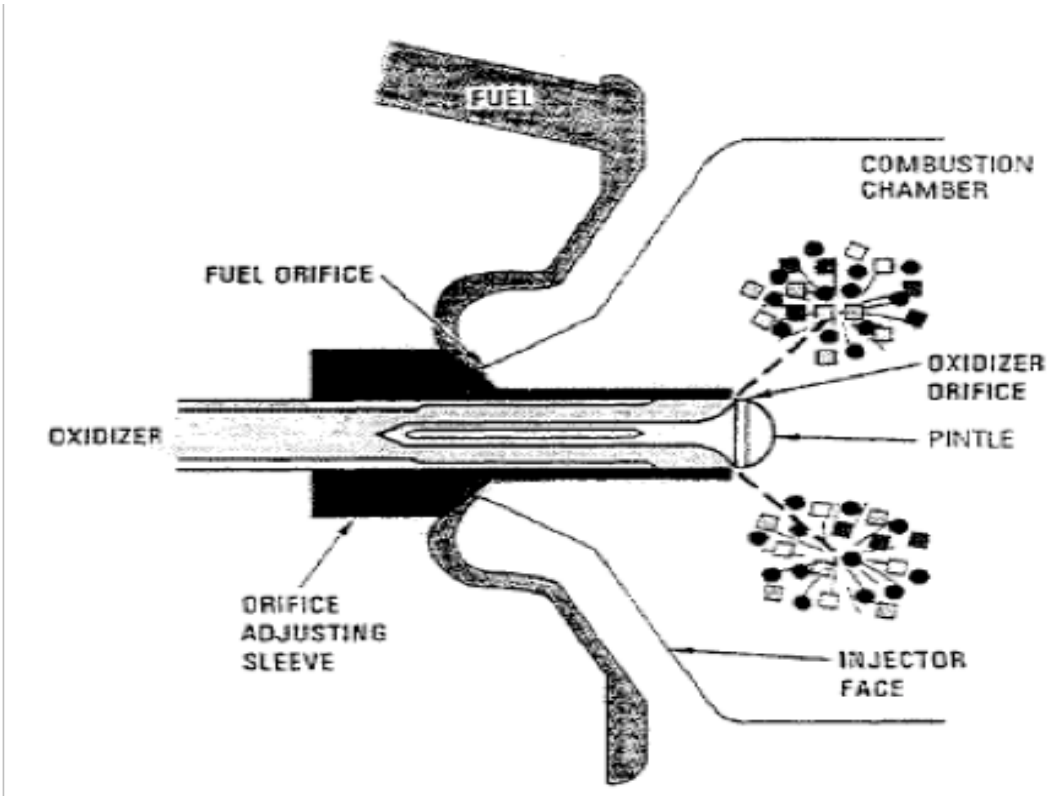

Figure 3.1: Pintle Injector[8]

sustainer engines. With lower thrust upper stage or landing engines that require deep throttling, additional throttling aids are often required.

3.1.3.2 Single Element Pintle Injector

The pintle injector is used in the LMDE engine. The pintle is a mechanically actuated piston that changes the propellant injection area for different thrust levels. This allows for precise control of the amount of propellants injected into the chamber, and is one of the reasons the LMDE was so successful. The pintle injector can also be used in a fixed thrust engine, with the added simplicity of eliminating the pintle actuation system. Since as few as five parts can be used for the injector assembly, the manufacturing and assembly of the injector can be quite simple compared to multi-element injectors.

With the pintle injector, one propellant is injected through a series of injection orifices in the center pintle piece. The other propellant is injected as an axial sheet concentrically around the pintle. It is essentially one large injection element, as shown in Figure 3.1. If the fuel is adequately sprayed toward the combustion chamber walls, it can both mix with the oxidizer and cool the inside wall of the chamber. One highly desirable feature of the pintle injector is its inherent combustion stability. Even at power levels as low as 10%, the pintle injector has never exhibited acoustic instability.[6] One downside to using pintle injectors is the relatively low combustion efficiency. It is common for recirculation areas to form at the base of the pintle. This can turn into a dead-flow region, and can cause some loss of efficiency. The chamber length must be designed to be long enough to allow for the propellants to mix adequately. The temperatures at the pintle tip need to be

evaluated, and the tip material must be selected so that the material does not melt with the high combustion chamber temperatures.

With these issues taken into consideration, pintle injectors typically do not exhibit the high efficiency that can be achieved with multi-element injectors. However, in some cases, it is worth taking the loss in efficiency in order to reap the benefits of the inherent combustion stability of this configuration for throttling applications.

3.1.3.3 Two or Multi-Stage Multi-Element Injectors

The idea of using two or multiple stage multi-element injectors takes advantage of the benefits of the high efficiency of the multi-element injector design and the area variation achieved using the pintle injector. Using several stages allows for certain stages or certain elements to be turned off at low power levels in an effort to keep the pressure drop over the injector high without having to put stringent requirements on the feed system. As mentioned previously, this is a relatively new area of research that is currently being investigated on MSFC's LLDET.

Some issues with multi-stage injectors include injector system complexity. Manufacturing a multi-element injector can be difficult, so manufacturing a system with multiple stages and valves to turn injection orifices on and off becomes more cumbersome. Also, the injectors that are turned off need to be purged so that hot combustion gases and propellants do not backflow into the injector orifices. However, if consistently good performance and feed system flexibility can be achieved, this could be an excellent option for use on a throttling engine.

3.2 Thrust Chamber

The thrust chamber consists of the volume between the injector faceplate and the throat where the combustion process takes place. In order to ensure that combustion stability is achieved, the thrust chamber must be designed such that the length is long enough to ensure proper mixing and combustion of the propellants. If the length is too short and the propellants exit the chamber without mixing and combusting, performance is lost. Combustion chamber volume is designed considering propellant mass flowrate, average specific volume, and the propellant stay time. Chamber length is often characterized as L^*, which is referred to as the "characteristic length." L^* is defined as

$$L^* = \frac{V_c}{A_t} \quad , \tag{3.1}$$

where V_c is the chamber volume and A_t is the throat area. As L^* is increased, the c^* also increases, to a limit. When choosing an appropriate L^*, one must consider the length available in the engine design envelope, the weight available for the combustion chamber, and how much c^* efficiency is actually needed to execute the mission. It also must be understood that increasing the L^* creates more surface area that needs to be cooled; thermal losses could increase. Larger L^* could also increase "the frictional losses in the combustion chamber, reducing nozzle stagnation pressure and resultant thrust."[5]

Chamber length also impacts the design of cold flow side, the fuel in the coolant tubes, particularly in expander cycle engines such as the RL-10. At low thrust levels, the mass flow rate of fuel pumped to cool the chamber decreases. As a result, the resonant time of the fuel in the regenerative tubes increases, and the fuel heats up more than at higher thrust levels due to increased heat transfer to the fuel through the tubes. In some cases,

fuel jacket boiling can occur. Fuel jacket boiling begins when the temperature rises above the critical temperature or when the pressure drops below the critical pressure of the fuel. This can either be driven by heat transfer or by a decrease in pressure due to lower flow rates. Thus, it is important for the fuel to stay above the critical pressure and below the critical temperature of the fuel. The reason fuel jacket boiling is undesirable is because it can lead to combustion instabilities. It can also impact the turbine performance since the turbine is just downstream of the coolant tubes. One way to avoid fuel jacket boiling is by using a flow control or venturi valve downstream of the coolant tubes. This can provide enough back-pressure at the low power levels to maintain pressures above the fuel critical pressure so that fuel jacket boiling can be avoided.

3.3 Turbomachinery

Turbomachinery systems for liquid rocket engines are very complex devices in terms of mechanical components and flow characteristic. They operate at very high speeds and have the potential to produce an enormous amount of power.

The RL-10 turbopumps are driven by a common fuel turbine. The LOX and fuel pumps are geared to achieve the proper mixture ratio of propellants. The mixture ratio, however, does not have to remain constant. On the CECE, the mixture ratio is varied by the use of an OCV that regulates the flow of oxidizer while maintaining fuel flow on the fuel pump. The TBVs used on CECE control the p_c and thus the power level while allowing the turbopump to remain above the stall region. The LMDE is quite simple in that it does not use turbopumps since it is a pressure fed engine. The LMDE uses flow control valves for the oxidizer and fuel feed systems.

Turbomachinery for throttling engines is designed for 100% thrust. When operating off the rated power level, special considerations need to be made for cavitation, rotordynamics, structural dynamics, bearings and fuel leakage flows, stall and velocity triangles, and surge.

3.3.1 Cavitation

Cavitation occurs when the local pressure at the blade is less than the vapor pressure of the fluid. "The term cavitation refers to conditions within the pump where, owing to a local pressure drop, cavities filled with…vapor are formed; these cavities collapse as soon as the vapor bubbles reach regions of higher pressure on their way through the pump."[22] The reason cavitation is undesirable is it can lead to structural damage and flow surges. Cavitation damage can be very difficult to eliminate and expensive to fix. It can decrease the performance of the pump, and impact the steady state and the unsteady or dynamic response of the fluid flow.[23] It can eventually lead to pump head fall-off, which is highly undesirable.

One method that is commonly used to characterize cavitation is called the "bucket curve," which shows the suction performance as a function of Q/N, where Q is the volumetric flow rate and N is the pump speed. As the engine is throttled to lower power levels, the pump characteristic Q/N decreases. The curve defines the boundary between cavitating and non-cavitating flow. As the pump operates below the bucket curve, less pump head is generated, and the pump moves into deeper cavitation zones. As the performance dips below the bucket curve, the vapor propagates down the blade, and the

blade becomes less effective and eventually ineffective. It is critical to understand this cavitation boundary as the flow coefficient is decreased at low power levels.

Another way to evaluate the system is by looking at the "knee curve," which shows the pump head rise as a function of cavitation number. As the cavitation number decreases, it eventually reaches a point where pump head can no longer be achieved. This is referred to as "head falloff." It is important to maintain a cavitation number that is greater than the head falloff cavitation number, with some margin.

3.3.2 Rotordynamics

Turbomachinery rotordynamics must be carefully evaluated for a throttling engine turbopump. It is critical to stay either above or below critical resonant modes of the turbopump. In order to assess the system, both linear and nonlinear rotordynamic analyses must be performed. During thrust ramp-up and ramp-down, moving through certain modes cannot be avoided; often times if the system moves through a mode relatively quickly, no effects are realized by the system. "Rotordynamic stability is another design issue requiring not only damping devices but also minimizing the destabilizing forces. Excessive vibration prevention due to unbalance, etc., is another design task. Gates for rotordynamic stability margins and vibration levels are required. The turbine can have the same kind of issues including disk mode instability, flutter of turbine blades, etc., which must be prevented and require gates as well. Bearing wear is also a design issue. The gate on bearings can be a trade between lifetime and maintenance (bearing replacement)."[24]

Rotordynamics consider the forces acting upon the turbomachinery components due to the rotating assembly, and interactions between the fluids and structural components. The

system responds through the bearings, and the system must be designed such that the bearings can withstand the loads at both high and low rotational speeds. Typically, the rotordynamic radial loads increase with speed, leading to wear and life concerns. The deflections also tend to increase with speed, leading to concerns about rub. "Operation of turbomachinery at or near a natural frequency causes excessive response, increases wear, and reduces reliability. Synchronous motion coincident with the rotor natural frequency is defined as operation at a critical speed. The dynamic response can be reduced by increasing the effective damping or designing the rotor to locate its natural frequencies far from the shaft-spin-speed excitation."[5]

At different speeds, different modes can be excited. The different modes impart different deflections on the shaft. These modes can be controlled through the design of the shaft assembly and the housing to ensure minimal deflections and to ensure adequate

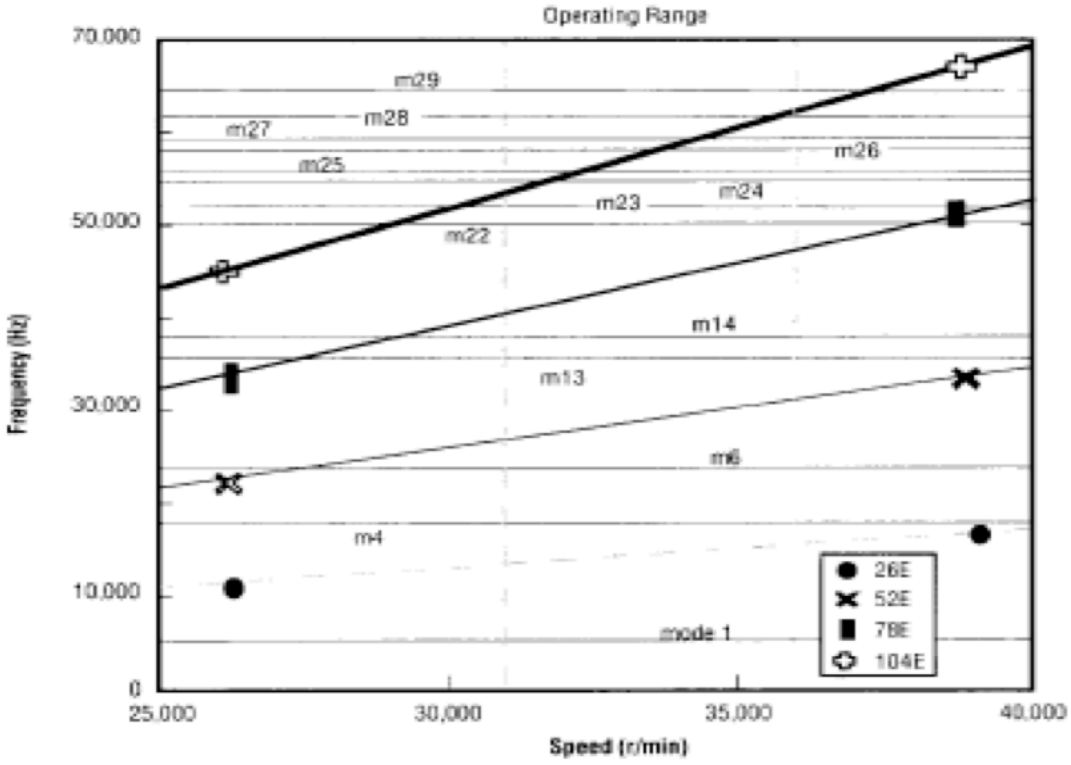

Figure 3.2: Campbell Diagram[26]

bearing life for the demands of a particular engine. This is typically accomplished by design the rotating assembly to operate below the critical speed. When throttling is needed, the operational speed range increases, and thus a greater range of modes need to be evaluated. Turbomachinery is balanced to the 100% thrust configuration, so when operating off this 100% thrust design point, sometimes additional instabilities from the rotor assembly can be experienced.[25]

The risk of encountering rotordynamic instabilities can be mitigated through proper material selection, the use of blade dampers to ensure proper damping of the structural modes, and appropriate shaft stiffness. Shrouds can also be added as stability aids.

3.3.3 Structural Dynamics

Structural strength requirements are critical for turbopump life considerations. The turbomachinery "must meet durability requirements that include low- and high-cycle fatigue, fracture, flutter/vortex shedding, acoustics, and creep."[24] If not designed correctly, the turbopump assembly can experience cracks, individual component failure, and fatigue failure.

Primary strength margins and low cycle fatigue limitations must be assessed. First, the operating speed ranges for flight are calculated. Then, the modes of all the components are calculated. Then, it is determined if the generated forces exceed the strength or excessively excite the modes of each part. These excitation intersections are usually shown in a Campbell Diagram where the modal excitation frequency vs. selected multiples of rotor speeds are identified. An example of a Campbell Diagram[26] is shown in Figure 3.2.

As an engine is throttled, a larger speed and frequency range needs to be evaluated. This poses some difficulties since it can be difficult to design around such a wide range of modes.

3.3.4 Bearings and Fuel Leakage Flows

As with the above mentioned turbomachinery components, the turbomachinery orifices and clearances are designed for full thrust. These flows and leakages control the amount of bearing coolant and the overall thrust balance of the turbopump. At reduced thrust levels, bearing leakages become a larger percent of the overall flow. As a result, pump efficiencies decrease as power levels are decreased.

One other consideration in this area centers around rotor speeds. As the pump speed decreases with power level, there is less radial growth of the rotating components. Thus, at lower power levels, clearances are increased, and pump efficiencies are decreased. This can also impact bearing coolant flow and turbopump thrust balance conditions, which can affect overall bearing life and manifest itself as turbopump vibration.[27]

3.3.5 Stall and Velocity Triangles

On the turbine side of the turbopump, it is important to achieve optimal efficiency, and to extract the optimal amount of work out of the driving fluid or gas. Typically, when designing a turbopump, the turbine blades are optimized to achieve the maximum amount of work through the series of turbine blades, both the rotor and stator blades, by designing to the angle of attack of the fluid. The “velocity triangles” refer to the net velocity vector of the fluid as it approaches the turbine blade, and the lift and drag components of that

vector. The velocity vector changes as it moves from the first stage turbine inlet vanes, to the first stage rotor blades, to the stator vanes, and so on. When an engine is throttled and a lower fluid velocity is injected into the turbine, the velocity triangles change, and in some cases efficiency is lost due to the now non-optimal attack angle relationship to the blade geometry.

It isn't likely that a turbine would be designed specifically for the low power levels. The approach that is typically taken is to design the blades to maximum thrust operation, and the performance that is achieved at low power levels is dealt with, and the efficiency losses are taken into account in the engine system model. Flow separation occurs when the flow momentum over the blades is reduced to a certain point; flow separation can lead to stall.[28] Flow separation from one blade causes a wake effect on the adjacent blade, which can lead to high loads and structural concerns. These wake effects can be compensated for by increasing the gap between the blades. Although increasing the gap reduces the blade loading, it can also lead to efficiency losses.

On the pump side, if the net velocity vector in a pump becomes too shallow, or if the ramp rate down to low power levels is too great, the pump can stall. Stall is more likely to occur on the pump side rather than the turbine side. On the turbine side, the main concern is losing efficiency. For deep throttling, the flow coefficient can fall far to the right of the head rise vs. flowrate graph, and can fall in the stall region. "The flow coefficient will fall substantially below its design value, the pump hydrodynamic flow will become highly unstable, efficiency will be poor, and greater inlet-suction pressure to the pump will be necessary to avoid cavitation."[29] It is also important to consider that when operating in a stall regime, the pressure oscillations can be nearly twice what they would be in a non-

stalled regime, and can be as high as five times nominal if operating in a cavitation regime.[29]

One way to compensate for velocity vector variation as the power level drops is to use a splitter vane to achieve better control over the fluid velocity vector as it enters the system.

For the RL-10 engine, the cavitating venturi valves are used in order to isolate the fuel pump from combustion chamber coolant oscillations, which also could lead to stall.[30] These combustion chamber coolant oscillations are caused by fuel jacket boiling, which is discussed in the combustion chamber section of this paper. The use of the valves in this instance keeps the pressure above the critical pressure of the fuel in the coolant tubes to avoid fuel jacket boiling. As boiling is avoided, the fuel can then drive the turbine without encountering stall. This is an excellent example of the combustion chamber, cavitating venturi valve, turbine, and both pumps all being an integrated system that requires careful system design.

3.3.6 Surge

Surge is another type of pump instability that is caused by "overall mass flow oscillations through the entire hydraulic system," which can "result in severe fluctuations in inlet and discharge pressures and mass flows."[31] It is desirable to avoid surge when possible. Surge can initiate upon reduced flowartes to the inducer, while maintaining a constant speed. Surge is a systems issue where the pump and other components interact in an unstable manner, leading to strongly coupled fluctuating flow.[28] This needs to be understood and avoided when designing a throttling turbopump.

3.4 Valves

Main valves and ancillary valves must be adequately designed to operate over a wide range of pressures and temperatures, while still maintaining the precision and control needed over the full operating range.

When designing both the valves and the valve actuators, considerations must be made to balance the pressures across the valve as thrust is decreased or increased. If the valve slew rates or sealing capabilities cannot accommodate the required throttle range, the engine could encounter difficulties with flow control that could impact all components.

The LMDE uses cavitating venturi valves on both the oxidizer and fuel feed sides in order to control the amount of propellant flow that reaches the injector. The use of these venturi valves allows for adequate force balance on the turbopumps and isolates the feed system from injection system effects. "As the pressure drop across the venturi throat increases, a critical point is reached wherein the total upstream pressure head is converted into velocity head and fluid vapor pressure. With the inlet temperature and pressure conditions held constant, a further decrease in the downstream pressure does not cause any change in the flow rate through the venturi."[32] At maximum thrust, the valve is noncavitating for a low pressure drop. As the engine is throttled (10-65% thrust in the LMDE), the valve operates in the cavitating range and achieves hydraulic decoupling.

As discussed in the combustion chamber section above, special valves can be used in order to provide enough backpressure just downstream of the coolant tubes in expander cycle engines such as the CECE. This is done in order to keep the fuel pressure in the coolant tubes above the critical pressure of the fuel.

On the CECE, turbine bypass valves are used to control the flow to the turbines. The flow bypasses the single fuel turbine in order to control the turbine speed. The amount of fluid bypassing the turbines is controlled by fuel turbine bypass valves (FTBVs).

3.5 Nozzle

The nozzle provides the necessary structure to react against the expansion of the combusted gas in order to pull as much work as possible out of the engine. The hot gases are accelerated through the throat and are expanded through the nozzle. Referring back to Equation (2.1), it can be seen that the relationship between exit pressure and exit area plays a role in the amount of thrust that is generated by the engine.

Nozzles can exhibit ideal expansion, over-expansion, or under-expansion. Ideal nozzle expansion occurs when $p_e=p_a$. Since in flight a rocket engine travels in a trajectory of changing altitude, and p_c is assumed to be constant for an engine operating at steady state conditions, ideal expansion only occurs at one altitude.

When the p_e is less than p_a, the flow is said to be over-expanded. When the p_e is greater than p_a, the flow is said to be under-expanded. This condition is undesirable, since the maximum amount of energy is not extracted out of the hot gas, and thus potential thrust is lost.

Flow separation is a function of "nozzle geometry, gas properties, characteristic Reynolds number, boundary layer displacement, boundary layer thickness, pressure gradients, wall temperature, and nozzle Mach number."[33] It is also a function of thrust ramp rate and wall temperature. Quicker ramp rates produce lower side loads. The method for nozzle cooling also impacts the type of nozzle separation that is experienced.

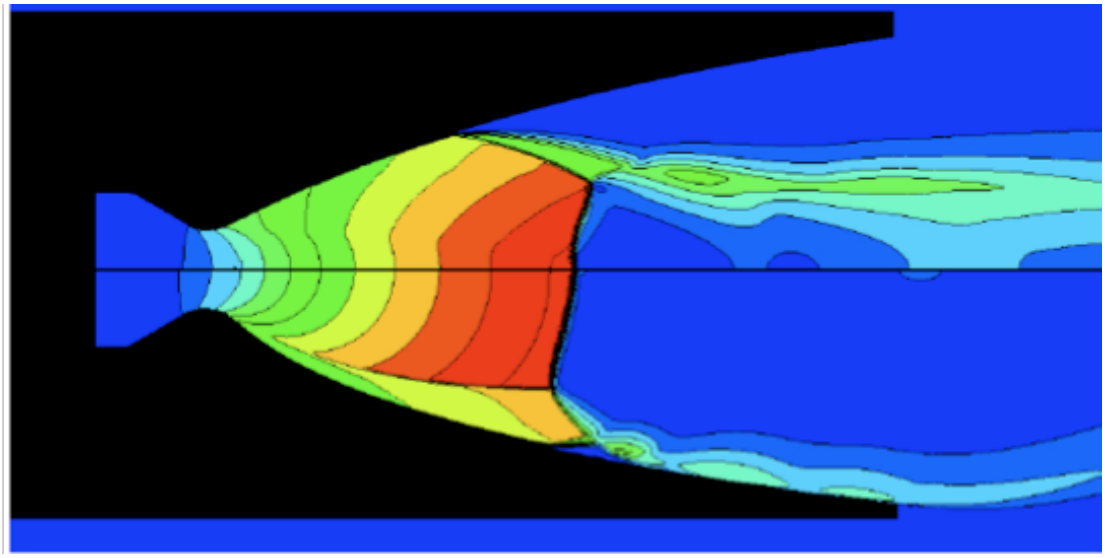

Figure 3.3: Free Shock Separation (top) and Restricted Shock Separation (bottom)[35]

Flow separation occurs when the exhaust gas detaches from the nozzle wall when the nozzle exit pressure is less than about 1/3 the ambient pressure into which the nozzle is discharging. Typically, if operating at steady state, nozzle flow separation is relatively symmetric. However, during engine transients and throttling, the separation can be asymmetric, and can impose significant side loads on the nozzle.[34] This is highly undesirable, but is unavoidable. Usually, a certain amount of flow separation can be tolerated; it needs to be determined on a case-by-case basis how much separation is acceptable to maintain structural integrity of the nozzle, engine, and test stand. As thrust is decreased and the flow separation moves up the nozzle, in extreme cases the throat can become un-choked, which leads to severe loss of engine performance.

Flow separation can be either Free Shock Separation (FSS) or Restricted Shock Separation (RSS). “The FSS occurs when the developing nozzle flow in the diverging section suddenly separates from the wall; since this is frequently non-axisymmetric, it will

induce a “side load”.”[35] “In RSS the separated flow reattaches to the wall; again, this is usually an asymmetric event.”[35] The FSS and RSS are shown in Figure 3.3.

One example where damage nozzle damage was observed occurred on an RD-120 engine, which is a Russian LH_2/LO_2, staged-combustion cycle engine that achieves a maximum vacuum thrust just shy of 195,000 lbf. “When the engine was throttled from 100% thrust to 25% thrust, the shock plane moved inside the nozzle to produce a vibration force 15-25 higher than when the engine runs at 100% thrust.”[36] 86 of the 480 metal fasteners holding the hatband stiffeners to the nozzle were found to be broken after the 25% thrust test.

3.6 Summary

Based on the discussions in this chapter, it is concluded that for the Mars lander engine, the following components are selected due their compatibility with throttling:

- An expander cycle is chosen for the engine due to its simplicity and reliability.
- A pintle injector is selected due to its inherent stability characteristics and ability to vary flow area to the chamber; this will be important for maintaining an acceptable $\Delta p/p_c$ at the injector.
- A thrust chamber is selected that has a long enough length to adequately pair with the pintle injector. The thrust chamber is regeneratively cooled, and must be long enough to allow for enough heat transfer into the fuel circuit to drive the turbines.
- Two independently driven turbopumps are chosen, one for the fuel and one for the oxidizer. The turbines are in series.
- Several valves are necessary; a thrust control valve is used to vary fuel flowrate to the turbines, and an oxidizer control valve is used to vary mixture ratio.
- The nozzle configuration is regeneratively cooled, and the shape is optimized for 100% thrust.

CHAPTER FOUR

DESIGN APPROACH

In this design approach, a mission is specified and initial requirements are established. Several assumptions are documented, which allow for a top-level design of a new throttling liquid propellant rocket engine.

The success criteria for this engine includes the following:

- Demonstrating a power balance model that closes.
- Demonstrating in a power balance model that a ratio of $\Delta p/p_c$ of 20% can be achieved at both 100% and 10% power levels using reasonable engine feed pressures and temperatures. "Reasonable" means the feed pressures and temperatures are within the American experience base for liquid rocket engines, which is 25-55 psia and cryogenic temperatures for a LOX-methane pump-fed engine.
- Achieving reasonable pump Δp, using reasonable pump speeds and turbine drive characteristics. Pump horsepower should be in the range of 2-400 Hp. It is expected that the fuel horsepower will be significantly higher than the oxidizer horsepower since the density of the oxidizer is greater than two times the density of the fuel.
- Achieving adequate cooling from the fuel in the regenerative cooling channels to keep the selected chamber material below its maximum allowed operating temperature.

- Achieving adequate temperature rise in the coolant fuel in order to successfully drive the fuel and oxidizer turbines to power the fuel and oxidizer pumps.

Additional design information, such as the turbomachinery detailed blade designs, specific valve design, and detailed injector and coolant channel design can be determined at a later date. For this study, success primarily includes achieving adequate steady state engine balance performance at both 100% and 10% power.

4.1 Design Tools

The design tools that are used in the design and analysis of this engine include Chemical Equilibrium in Excel (CEQUEL®), Chemical Equilibrium with Applications (CEA), ISP CEA Model, and the power balance model that is developed during this activity. ISP CEA Model is a code that was developed by Joe Leahy at Marshall Space Flight Center in 2006. It runs with CEQUEL, and while CEQUEL can provide for predicted combustion chamber characteristics, ISP CEA Model adds in various component efficiencies to allow for a more realistic estimate of the combustion chamber parameters. There is a high degree of confidence in the predictions for combustion chamber performance since ISP CEA Model results compare very well to actual test data for SSME, J-2X, RL10, CECE, and RD-180. Various web-based tools are also used to aid in unit conversions and in thermo-chemical property determinations. Google SketchUp is used to model the combustion chamber and nozzle assembly and the engine schematic.

Several textbooks are used as guidelines for the design of the engine. In particular, "Design of Liquid-Propellant Rocket Engines" by Dieter K. Huzel and David H. Huang,[5]

"Rocket Propulsion Elements" by George P. Sutton and Oscar Biblarz,[37] and "Space Propulsion Analysis and Design" by Ronald W. Humble, Gary N. Henry, and Wiley J. Larson[38] are quite useful.

In addition to using textbooks and combustion prediction programs, discussions with many professionals at NASA Marshall who have many years of experience designing liquid propellant rocket engines are extremely helpful. In many cases, assumptions are made based on historical performance of engines similar to the engine designed in this study.

4.2 Overall Design Approach

The overall design approach for this activity is outlined in Figure 4.1. A mission assessment is performed, and preliminary thrust and engine sizing requirements are established. This mission assessment is based on several preliminary Mars landing studies that have been performed by NASA.[39] Once the thrust range is established, the propellant selection is made. Educated estimates are made of the parameters outlined in Table 4.1, including chamber pressure, c^* efficiency, c_f efficiency, nozzle area ratio, and mixture ratio. Holding all parameters except mixture ratio constant, a trade study is performed in order to select a mixture ratio that will allow for optimal engine I_{sp} at each power level. Once the preliminary input parameters are selected, ISP CEA Model is run in order to produce combustion chamber parameters such as I_{sp}, thermodynamic properties of the combustion gas, preliminary chamber sizing, and propellant flow rates. After the equilibrium calculations are complete, an engine schematic is drawn to reflect the general flow routes through the engine.

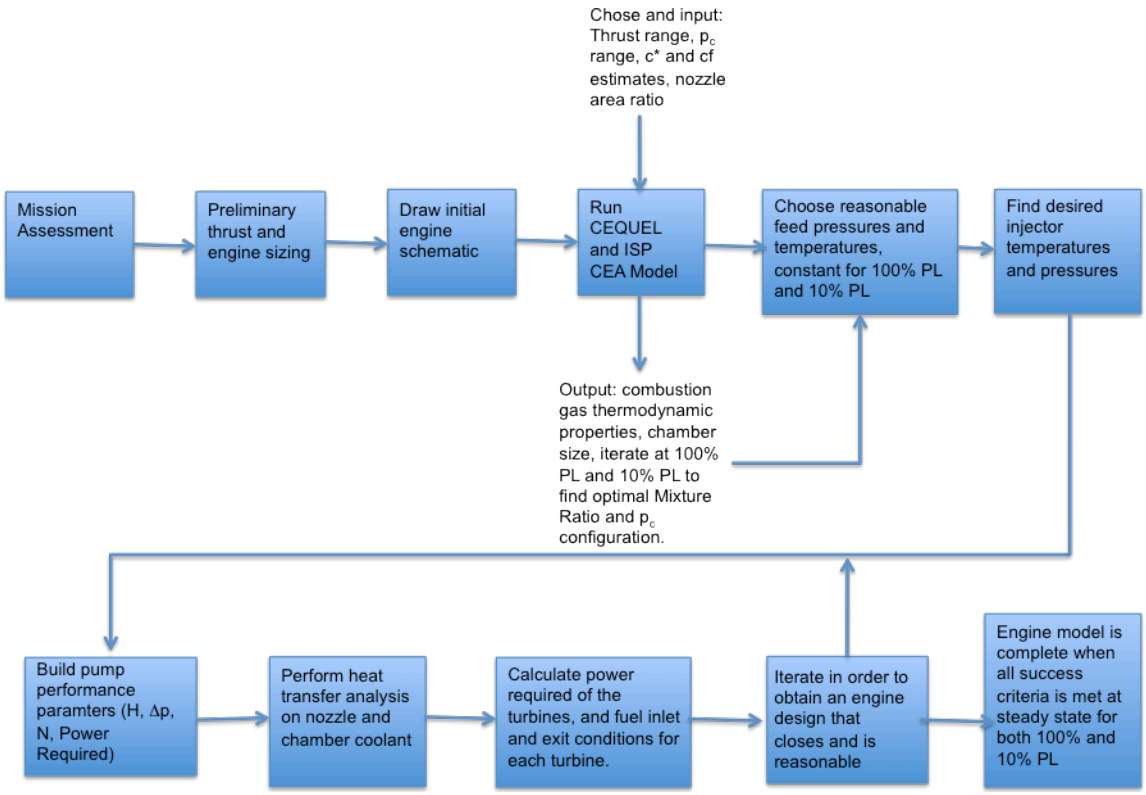

Figure 4.1: Overall Engine Design Approach

After the ISP CEA Model output parameters are found, component sizing begins. All component sizing is performed using the 100% power level. Then, 10% power level operating parameters are determined using the engine geometry that is set by the 100% power level, with the exception of the injection area, which is variable. Initially, some research is performed on existing engine feed systems to determine a reasonable feed pressure and temperature for both the fuel and the oxidizer. At the combustion chamber end, the injector pressure and temperature are found for the fuel and oxidizer by setting $\Delta p/p_c$ to 20% for both 100% and 10% power. Next pump pressure and temperature rise is calculated for the oxidizer pump, followed by pump calculations for the fuel pump.

Educated estimates are made here based on engines in a similar thrust class, and iterations are performed throughout the design process in order to obtain pump parameters at both power levels. A heat transfer analysis is performed on the regenerative coolant tubes of the nozzle and chamber, and a pressure drop and temperature rise in the fuel is calculated. The maximum wall temperature is also calculated and compared to the temperature limitations of the chosen wall material. Using the results from the heat transfer analysis, the drive power that is generated by the fuel is calculated for both the fuel and oxidizer turbines. Excess fuel is routed directly into the combustion chamber, while a portion is used to cool components such as pump and valve bearings. If the turbines have enough power to drive the pumps, and the desired injection feed parameters are achieved, then the engine design is considered to be feasible.

4.3 Preliminary Design Decisions

In order to begin designing a deep throttling liquid rocket engine for a Mars lander application, several design decisions need to be made, including propellants, thrust, chamber pressure, engine cycle, injector, and turbopump configuration.

As stated above, the propellant selection has been specified in the engine requirements. LOX-methane is a sound choice for propellants for this application, as both oxygen and methane are prevalent on the Martian surface. In addition, a fairly high I_{sp} can be achieved using methane, and its density is desirable for easy storage in small tanks, compared to what would be required for liquid hydrogen. One difficulty with methane is that sometimes it can be difficult to ignite. So, if relying on LOX-methane for a return mission, it would be desirable to have redundant ignition systems. When using methane as

a propellant, it is also important to factor in the loss in heat transfer in the nozzle region due to Carbon deposits. Carbon deposition "typically occurs at locations of the highest heat transfer, such as just upstream of the nozzle throat."[34] This carbon layer can impede the heat transfer process, raise the inner wall temperature, and can cause failures.

The thrust has been defined in the mission requirements as spanning from 1,500 lbf to 15,000 lbf. This can be achieved, and to keep the engine size down, chamber pressures from 80 psia to 800 psia have been chosen.

Based on the success of the RL-10 engine family, the expander cycle is chosen. The simplicity and reliability of the expander cycle is desirable for a Mars mission, and its performance is adequate for an engine within this chosen thrust class. As the RL-10 has been run using LOX-methane propellants in addition to its standard LOX-hydrogen propellants, it is believed that methane will perform adequately using an expander cycle.

For this application, a pintle injector is chosen due to its inherent stability characteristics, and its ability to vary the flow area at different power levels. Although mechanical actuation devices are required, and the injector efficiency will be somewhat lower than a multi-element injector, the stability, reliability, and historical success drives the selection of the pintle injector. The variable pressure drop over the injector is also highly desirable for a deep throttling application.

The turbomachinery configuration chosen for this study is dual, independently driven LOX and fuel turbopumps. There are two bypass legs; one allows the fuel to bypass both the fuel and oxidizer turbine to control turbine and pump speeds. A second bypass leg is added after the fuel turbine, before the LOX turbine in order to provide the ability to control the mixture ratio. The oxidizer control valve is used to control how much fuel

bypasses the oxidizer turbine, thus controlling the amount of oxidizer that is pumped into the combustion chamber. The dual independent turbine configuration is somewhat of a concern since the fuel that drives the turbines will need to have enough energy coming out of the regenerative cooling tubes in order to drive both a fuel and an oxidizer turbine to meet the fuel and oxidizer pump requirements.

Throttling of this engine is achieved by using the thrust control valve, directly downstream of the coolant jacket, to redirect a portion of the fuel flow in order to decrease the fuel and oxidizer turbine drive speeds. The pintle injector is used along with the thrust control valve in order to vary the injection area of the fluid that enters the combustion chamber. This allows for control of the $\Delta p/p_c$ across the throttling range. In addition to the TCV and OCV, there is a main oxidizer valve (MOV) and a main fuel valve (MFV) to turn the fuel and oxidizer supply on or off.

A schematic showing the overall Mars lander engine cycle is shown in Figure 4.2. The schematic is highly simplified. It does not show the pneumatic system for valve and pintle injector actuation or a Helium purge system. It also does not show the electrical system for the engine. These systems would have to be designed at a later date when more detail can be added to the engine design. This study focuses on the propellant flow system, and the pressures and temperatures are specified at each defined critical point (O1, F2, etc.). Overall turbopump performance and injector performance is discussed in later sections of this paper.

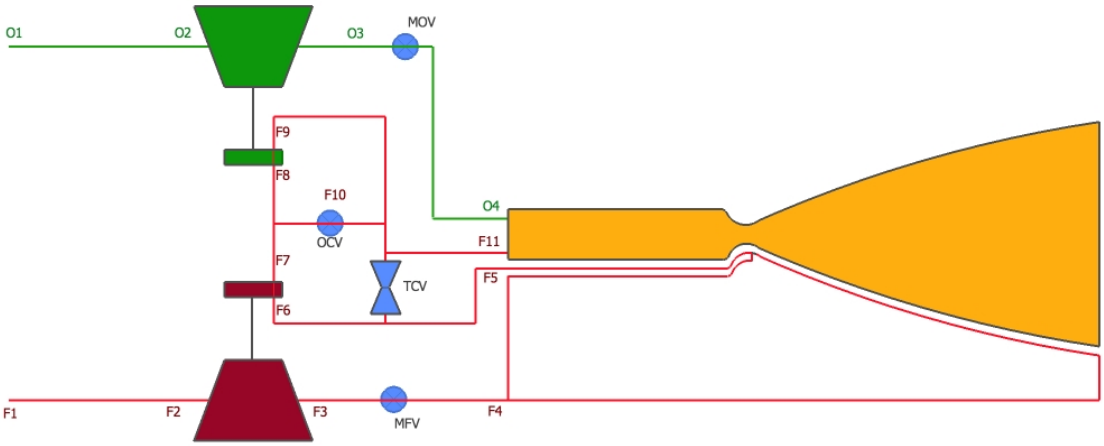

Figure 4.2: Mars Lander Engine Schematic

CHAPTER FIVE

RESULTS AND DISCUSSION

This chapter provides a discussion of the analytical results for the assessment performed on the engine configuration defined in Chapter Four. It includes the initial mixture ratio trade and determination, chamber design, injector design, pump design, regenerative coolant chamber design, and turbine design.

5.1 Mixture Ratio and Preliminary Performance Determination

In order to begin the study of the performance of this engine, it is necessary to choose

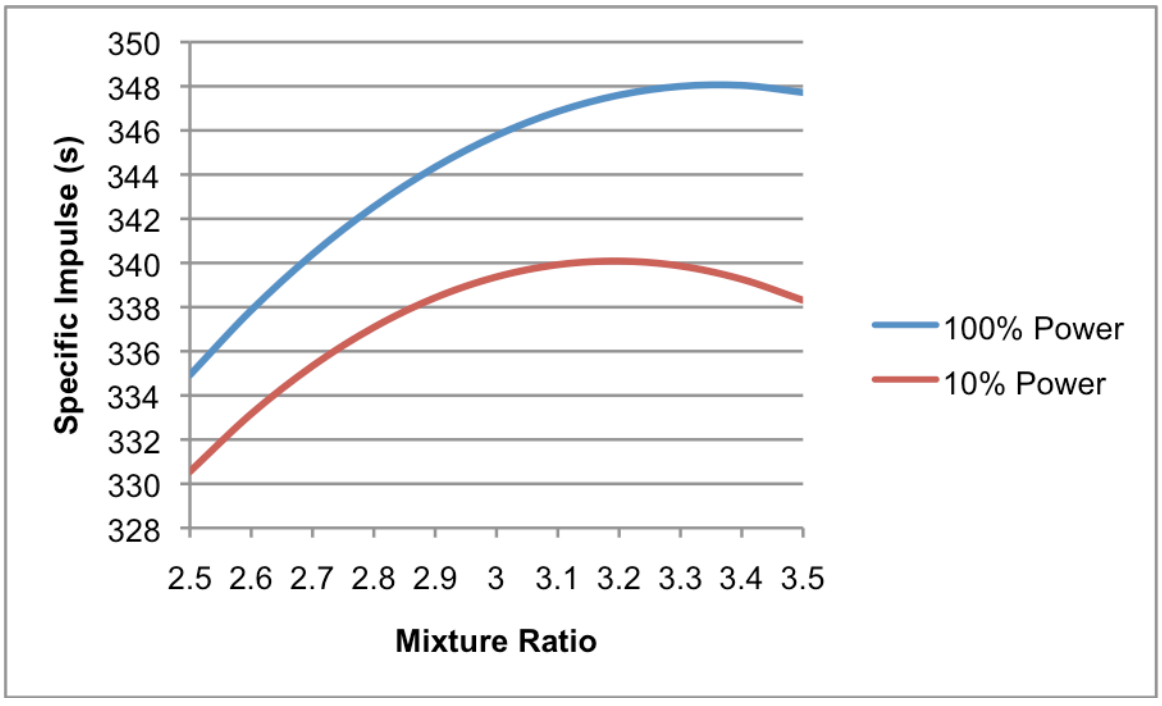

Figure 5.1: Specific Impulse vs. Engine Mixture Ratio

an optimal mixture ratio that the engine will operate at. ISP CEA Model is used in order to run a parametric study on I_{sp} as a function of mixture ratio at both power levels, as shown in Figure 5.1. Resulting from this parametric study, a mixture ratio of 3.3 is chosen for both power levels, although in reality, better performance may be achieved using a mixture ratio closer to 3.4 at 100% and 3.2 at 10% power. Mixture ratio adjustments are made using the oxidizer control valve on this engine.

Once the mixture ratio is established at each power level (PL), ISP CEA Model is used to determine the combustion characteristics of the mixture. The inputs to ISP CEA Model are shown in Table 5.1. A portion of the critical output parameters that are useful to this study are shown in Table 5.2. Performing this analysis using CEA ISP Model provides for a reasonable starting point in designing the engine power balance.

It is noted that a 96% c_f efficiency is chosen for 10% power, whereas a 97% c_f efficiency is used at 100%. A 97% c_f efficiency is chosen at 100% power since this is a

Table 5.1: CEA ISP Model Inputs

Parameter	100% PL	10% PL
Fuel	CH4 (G)	CH4 (G)
Oxidizer	O2 (L)	O2 (L)
Chamber Pressure (psia)	800	80
Chamber Mixture Ratio	3.3	3.3
Nozzle Area Ratio	40	40
Engine Thrust (lbf)	15000	1500
c* Efficiency	97%	97%
c_f Efficiency	97%	96%

Table 5.2: CEA ISP Model Outputs

Parameter	100% PL	10% PL
Actual Vacuum Isp (s)	349.34	341.06
Actual C* (ft/s)	5910.21	5755.98
Actual Cf, vacuum	1.90	1.91
Exit Plane Pressure (psia)	2.01	0.22
Combustion Chamber:		
Combustion Temperature (R)	6377.39	5830.74
Molecular Weight (lb/mol)	21.22	20.61
Enthalpy (Btu/lbm)	-600.85	-600.85
Ratio of Specific Heats	1.13	1.12
Cp (Btu/lbm-R)	1.74	2.43
Overall MCC/Noz Eta	0.94	0.93
Aero Throat Area (in^2)	9.86	9.84
Exit Diameter (in)	22.41	22.38
Chamber Area (in^2)	19.73	19.68
Chamber Diameter (in)	5.01	5.01
Total Eng Flow (lbm/s)	42.94	4.40
Total Fuel (lbm/s)	9.99	1.02
Total Lox (lbm/s)	32.95	3.38
% Fuel	0.23	0.23
% Lox	0.77	0.77

typical value that provides for the right correction factors in predicting the correct nozzle performance parameters. A slight 1% decrease moves the c_f efficiency to 96% at 10% power to provide for a reasonable estimate of throttled performance, based on predicted vs. test results that are observed for similar engines. This is due to increased nozzle efficiency losses at low power levels, due to non-optimal expansion, which plays a role in lowering the specific impulse at low power levels. A plot of specific impulse vs. c_f efficiency is shown in Figure 5.2.

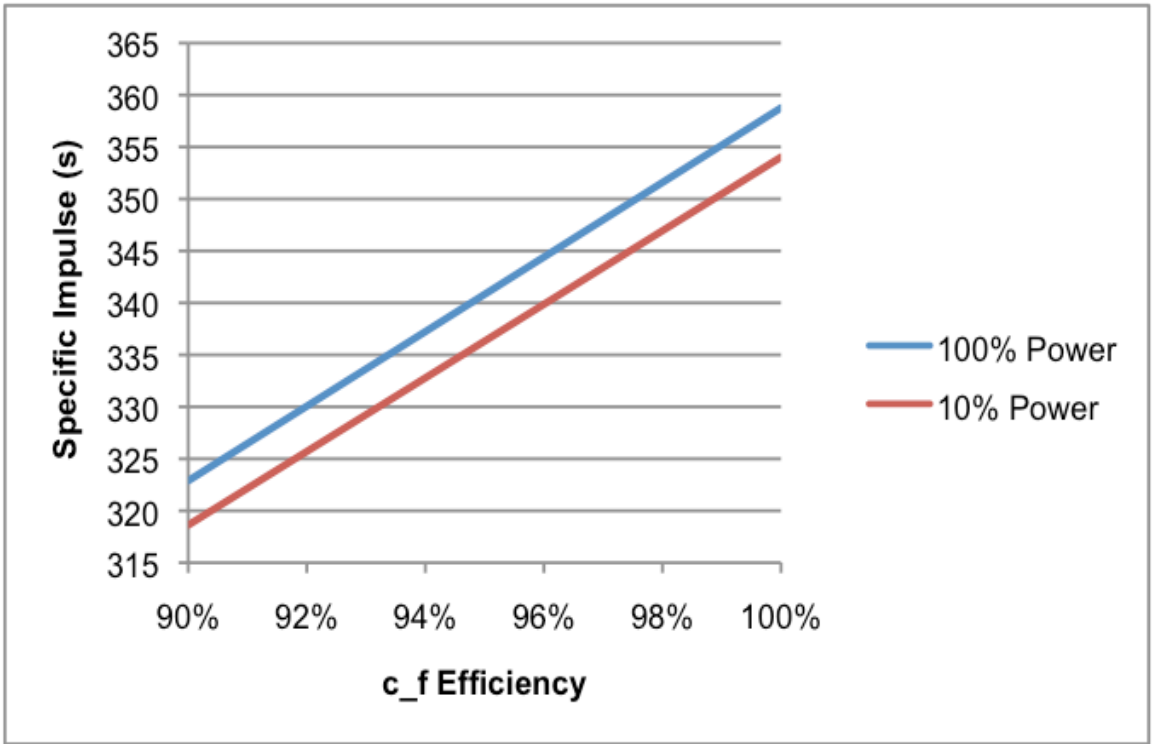

Figure 5.2: Specific Impulse vs. c_f Efficiency

5.2 Overall Engine Power Balance

The overall engine power balance results are displayed in Appendix A. The engine inlet parameters are set based on previous engine experience, which indicates that the inlet pressures should range from 25-55 psia, and the inlet temperatures should be cryogenic.

The engine oxidizer inlet temperature is 163 R and the inlet pressure is 45 psia. The fuel inlet temperature is 172 R and 45 psia. The inlet conditions remain constant over the engine throttling range.

5.2.1 LOX Circuit

The oxidizer flows through the oxidizer inlet duct and into the oxidizer turbopump, where the head increase is 1945 ft at 100% power and 174 ft at 10% power. The details of the oxidizer turbopump design are discussed in Section 5.5.1. After the oxidizer exits the oxidizer pump, it flows through the main oxidizer valve and into the LOX injection manifold. The oxidizer reaches the injector inlet at 960 psia and 170 degrees R at 100% power, and at 96 psia and 170 degrees R at 10% power. The methodology that is used for determining the injector pressures and temperatures is discussed in Section 5.4. The pintle injector area is adjusted accordingly based on the operating power level in order to create a roughly 20% pressure drop from the injector inlet to the combustion chamber. This is required to achieve combustion stability at all power levels.

5.2.2 Fuel Circuit

The fuel circuit is more complex than the oxidizer circuit, since the fuel is fed through the fuel turbopump, pumped through the regenerative coolant tubes, where the fuel is heated and picks up energy in order to drive both the fuel and oxidizer turbines before it is pumped into the fuel manifold for injection into the combustion chamber. The fuel feed temperature and pressure is chosen to be 172 degrees R and 45 psia. These parameters are

chosen with the expectation that the fuel will be delivered to the fuel injection manifold at a temperature of 180 degrees R and at a pressure of 960 psia at 100% power and 96 psia at 10% power.

5.3 Thrust Chamber Design

The first component to be designed is the thrust chamber, which is sized to the 100% power level. The 10% power level calculations all use the same geometry that is set with the 100% power level calculations. Understanding the outputs from the ISP CEA Model provides for a starting point for the thrust chamber design. One of the inputs into ISP CEA Model is contraction ratio, which is equal to the chamber area divided by the throat area. Since the throat area and contraction ratio are known, the chamber area can be determined. The chamber volume can be determined by choosing a chamber length of 24 inches, and multiplying the chamber length by the chamber cross-sectional area. A length of 24 inches is a little long in comparison with similar engines with a throat diameter of approximately 3.4 inches;[5] however, since this engine uses a pintle injector and an expander cycle, it is determined that a longer chamber is better in order to provide enough space for propellant mixing and for more complete combustion to occur, and to allow time for the coolant to heat up in the throttled configuration in order to be able to gain enough energy to drive the fuel and oxidizer turbines. The characteristic length is found by dividing the chamber volume by the throat area; this value comes out to 48 inches, which is typical for a LOX-hydrocarbon engine chamber.[5]

Preliminary analysis of the nozzle contour follows the chamber geometry assessment. An area ratio of 40 is chosen, and the nozzle exit and throat radii are known from ISP

CEA Model outputs. For simplicity in this study, the nozzle shape is a simple bell shape, and initial approximations assume a nozzle half angle of 15 degrees and a throat contour radius equal to the radius of the throat. The nozzle half angle is defined as the initial angle between the nozzle wall and the centerline of the nozzle. Using these parameters, the nozzle length is calculated to be 35.3 inches. The nozzle geometry is used in calculating the length of the coolant tubes for regenerative cooling of the nozzle and thrust chamber. Figure 5.3 shows a drawing and 3D model of the engine thrust chamber and nozzle.

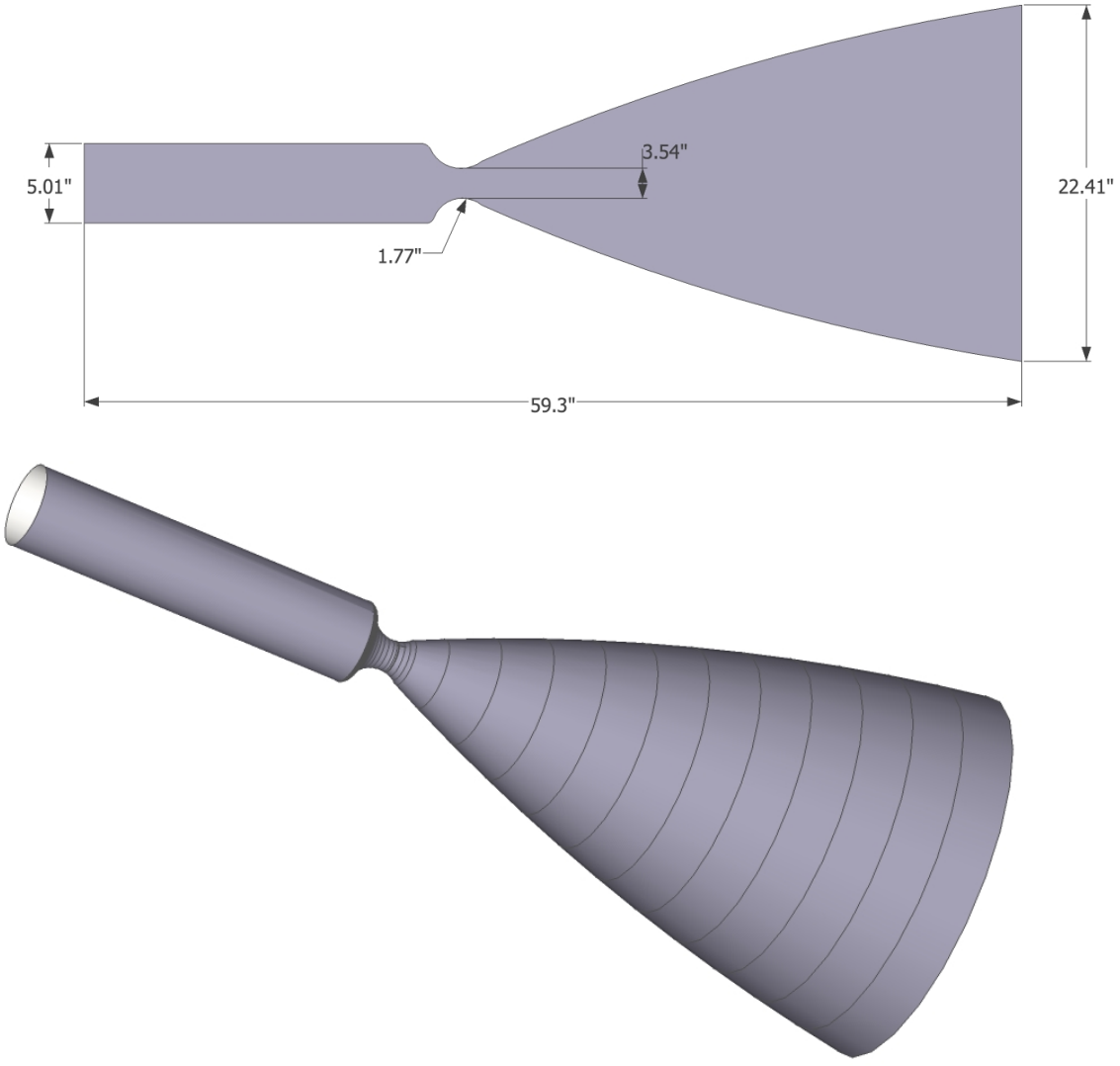

Figure 5.3: Mars Lander Engine Thrust Chamber and Nozzle

5.4 Injector Design

As stated earlier, the injector for this design is a pintle injector, which allows for real-time injection area adjustment so that adequate values of $\Delta p/p_c$ can be achieved without driving the feed system requirements up to a point where they would be unreasonable to achieve. Having $\Delta p/p_c$ greater than 15% is critical in order to achieve combustion stability. That being said, the injector Δp is determined by setting $\Delta p/p_c$ to a conservative 20% for both the 100% and 10% power level cases, and solving for Δp. Assumptions are made on the injection temperatures of both the fuel and oxidizer, and densities are found at the injection temperatures and pressures. Knowing the mass flow rates, densities, and estimating a head loss coefficient, the injection areas can be found using the equation

$$A = \dot{w}\sqrt{\frac{2.238K}{\rho\Delta p}} \qquad .^{5} \tag{5.1}$$

The injection area for the fuel side is found to be 8.94 in^2 for 100% power level and 2.87 in^2 for 10% power level. The injection area for the oxidizer side is found to be 8.22 in^2 for 100% power level and 5.94 in^2 for 10% power level. There is a high level of confidence in the injection areas that are calculated for the injector, however the selection of a different head loss coefficient could impact the results.

The injector inlet requirements along with the propellant feed requirements drive the design of the turbopumps. The fuel needs to be delivered to 960 psia at 180 degrees R, and the oxidizer needs to be delivered at 960 psia at 170 degrees R at 100% power in order to achieve combustion stability and the thrust required. At 10% power, the fuel temperature and pressure are 96 psia and 180R, and the oxidizer temperature and pressure are 96 psia and 170R.

As this is simply a preliminary performance assessment, much more detail needs to follow in the area of injector design. The contour of the pintle injector, the material selection, and the actuation features all require further definition. Testing is necessary in order to determine the true head loss coefficient for a more accurate prediction on the injection area required at each thrust level.

5.5 Turbopump Design

In order to design the turbopumps, it is first important to evaluate the pump performance that is required of the engine, followed by the turbine performance required to drive the pumps. Some iteration is required during the design phase, in particular on the fuel pump, since the fuel pump is responsible for pumping the fuel through the regenerative cooling tubes and through the fuel and oxidizer turbines. The overall performance parameters for both the oxidizer and fuel pumps are displayed in Table 5.3.

Table 5.3: Mars Lander Engine Pump Performance Parameters

Parameter	Ox Pump		Fuel Pump	
	100% PL	10% PL	100% PL	10% PL
p_{feed} (psia)	45	45	45	45
p_{inlet} (psia)	44	44	44	44
T_{inlet} (R)	163	163	44	44
$p_{discharge}$ (psia)	1008	101	2000	1155
$T_{discharge}$ (R)	171	164	181	181
Δp_{pump}	964	57	1956	1111
Q (gpm)	63	21	161	17
ΔH (ft)	1945	174	5987	5740
N (rpm)	36968	8250	53607	36000
η_p	60%	40%	64%	43%
P_P (Hp)	58.87	2.67	170	25

5.5.1 LOX Pump Design

The LOX pump is fairly easy to define, since the entire LOX circuit consists of a feed line, a LOX pump, a main oxidizer valve, and the LOX side of the injector. Thus, by estimating the expected losses in the feed lines and across the main oxidizer valve, it can be determined what head rise needs to be delivered by the pump, what the rotational speed needs to be, and the horsepower that is required to drive the LOX pump. As stated earlier, the feed parameters are determined to be 45 psia and 163 degrees R. There is a small amount of pressure loss in the inlet ducting, so the feed pressure is multiplied by 97% to estimate the pressure delivered to the pump inlet, which is 43.65 psia. The volumetric flowrate of the pump is found by dividing the mass flow rate by the density of LOX. This value is found to be 0.14 ft^3/s at 100% power and 0.0472 ft^3/s at 10% power. When transitioning between power levels, the feed parameters remain unchanged, while the mass flowrates do change. The required change in pressure across the pump is 964 psia at 100% power level and 57.15 psia at 10% power level. The discharge pressure on the oxidizer side is determined by multiplying the required pressure at the injector by 5% to account for losses in the feed system between the pump discharge and the injector inlet.

Calculating pump performance at throttled power levels requires the use of generalized pump maps and a bit of iteration in order to achieve pump speeds and pump powers and efficiencies that are reasonable. In order to use pump maps, the head coefficient and flow coefficient must be determined at the primary power level. Normalized head and flow coefficients must be determined in addition to design head and flow coefficients at primary power level. The equations used for head and flow coefficient

calculations are

$$\psi_N = \frac{\Delta p}{\rho N^2} \times \frac{1}{\psi_D}, \text{ and} \tag{5.2}$$

$$\phi_N = \frac{\dot{m}}{\rho N} \times \frac{1}{\phi_D}, \tag{5.3}$$

where Δp is pressure rise through the pump in psia, φ_N is the normalized head coeffieicnt, φ_D is the design flow coefficient, N is the pump speed in radians per second, ρ is the fluid density in lb_m/ft^3, ϕ_N is the normalized flow coefficient, and ϕ_D is the design flow coefficient. In order to use Equations (5.2) and (5.3), the pump speed is needed. The density of LOX, the flow rate, and the pressure rise is known. The pump speed is determined from the equation

$$N = \frac{\Delta H S^{.75}}{Q}, \tag{5.4}$$

where ΔH is the pump head rise in ft, S is the pump specific speed, and Q is the volumetric flowrate in gpm. In this case, S is estimated to be 1000, and Q is calculated from the mass flow rate and density of LOX. The pump head rise is calculated from the Δp required and the LOX density.

As all parameters are now known at the 100% power level, the normalized head and flow coefficients are assumed to be 1. Thus, the design head and flow coefficients can be calculated. The design head and flow coefficients remain constant over the thrust range. At 10% power, a new normalized flow coefficient can be calculated based on the new propellant density and LOX flowrate. A 10% power level speed is guessed initially. The value for ϕ_N at 10% power can be calculated. Using the pump map, a new φ_N can be determined, and Equation (5.2) can be used to calculate the pressure rise available over

the pump using that value for N. Iteration on N and ϕ_N is required in order to reach the desired pressure rise at 10% power. The generic pump map and a sample calculation can be found in Appendix B.

A pump efficiency of 60% is chosen at 100% power level, and 40% is chosen at 10% power level due to expected losses in the pump efficiency in the highly throttled configuration. In reality, once the pumps are designed, test data will provide for a true reading of pump efficiency. For this systems study, the efficiency is assumed to be within family of historical pumps in this thrust class. The power required of the pump is determined using the following equation,

$$P_P = \frac{\rho Q \Delta H}{\eta_P}, \tag{5.5}$$

where P_p is the power required of the pump in horsepower, ρ is the fluid density in lbm/ft^3, Q is the volumetric flow rate in ft^3/s, and η_p is the pump efficiency. A conversion factor of 1/550 is required to achieve the power in horsepower. The pump power required is 58.86 Hp at 100% power, and 2.67 Hp at 10% power. The power requirement is critical in determining the turbine performance requirements for this turbopump.

Since oxygen is a common liquid rocket engine propellant, the performance data on the oxidizer pump can be compared to the oxidizer pump on J-2X, and RL-10 CECE. Even though the J-2X engine has a much higher thrust than the Mars lander engine, the J-2X oxidizer pump performance characteristics can be used to validate the Mars lander engine and power balance model calculations. The J-2X inlet and exit parameters and the predicted J-2X oxidizer pump efficiencies are input into the Mars lander power balance model. The resultant pump speeds and power required from this model match very well with the pump speed and power required in the governing power balance model for J-2X.

For the pump speed, the specific speed of the pump can be adjusted in order to bring the results from this model even closer to the J-2X predicted performance. A similar comparison is made using RL-10 CECE oxidizer pump inputs, and again, there is good agreement with the CECE power balance model.

It is noted that the pump speeds achieved in this study for the Mars lander engine are a bit high; this is primarily due to the selection of specific speed of the pump. This value can eventually be adjusted when the internal design of the pump is defined in more detail.

5.5.2 Fuel Pump Design

The fuel circuit is more complex than the oxidizer circuit, so the fuel pump performance requirements are greater than the requirements of the LOX pump. As discussed earlier, the requirement is for the fuel to arrive at the injector inlet at 960 psia and 180 degrees R for 100% power, and at 96 psia and 180 degrees R at 10% power.

The fuel pump discharge pressure is chosen to be 2000 psia at 100% power and 1155 psia at 10% power. The discharge temperature is chosen to be 181.3 R at both 100% and 10% power. These values are chosen based on experience, and based on iteration with the coolant flow circuit, which is discussed in Section 5.6.

Once the fuel pump inlet and discharge pressures and temperatures are determined, calculations very similar to the ones stated in Section 5.5.1 for the LOX pump are performed. One notable difference between the LOX pump and the fuel pump is that the fuel pump is a 2-stage pump. The first stage discharge temperature and pressure becomes the second stage inlet temperature and pressure. Each pump stage is treated individually. The pressure rise of each stage is calculated, along with fluid densities, flow rates, and

pump speeds. The higher speed that is determined from the two stages becomes the overall pump speed. After the 100% power level pump speed is determined, the 10% pump speed is determined in the same fashion as the LOX pump by iteration using the generalized pump maps.

One finding that is worth noting is that on the fuel pump at 10% power, the relative contribution of the first and second stage pumps does not correlate to the pressure rise contribution of each stage at 100% power. At 10% power, when iterating on pump speed, the pressure rise is calculated for each stage individually, but an eye is kept on the total pressure rise over the entirety of the 2-stage pump. It is discovered that the second pump stage has a greater contribution to the overall pressure rise at 10% power than it does at 100% power. At 100% power, the first stage contributes 58% of the overall pressure rise, while at 10% power, the first stage contributes 41% of the overall pressure rise.

In terms of validating the results of the fuel pump calculations, there is not methane pump performance data readily available. However, since the same calculations are used on the fuel side that were used on the oxidizer side, and the oxidizer pump calculations have been compared to the J-2X and CECE oxidizer pump calculations, it is believed that the fuel pump calculations are also reasonable.

5.6 Regenerative Coolant Chamber Design and Heat Transfer Analysis

The regenerative coolant system is designed next. This system consists of methane fuel, which flows through the coolant tubes in order to cool the thrust chamber walls. There are two primary design goals for the regenerative cooling system; it is critical that the combustion chamber wall is kept at a temperature below the yield temperature of the

material, and it is critical that the coolant picks up enough heat upon exiting the coolant tubes in order to have enough velocity and enough energy to drive both the fuel and oxidizer turbines. This section is simplified significantly in order to achieve overall performance requirements. The tubes are assumed to be a constant diameter, which in reality is not true. The tubes would actually vary in diameter in order to provide a fit both at the throat, around the nozzle, and around the combustion chamber. For this case, 1.5 tube passes are assumed, and the heat transfer analysis is focused at the throat area. Also, first order "bulk" properties are calculated in this section, rather than transient properties. This is done in order to simplify the model. A more detailed analysis is required for future evaluation of the coolant heat transfer section of this engine.

Initially, a material X-750 is chosen for the regenerative cooling thrust chamber due to its high strength and recommended use with hydrocarbon propellants. The material X-750 has a maximum temperature limit of 1460 degrees R, so it is a requirement to keep the wall temperature well below 1460 degrees R. The material properties are pulled for this particular material in order to evaluate its heat transfer capabilities using methane as a coolant.

There are a few, fairly simple equations that are outlined in "Modern Engineering for Design of Liquid-Propellant Rocket Engines" by Dieter K. Huzel and David H. Huang.[5] These equations are used for the heat transfer analysis of the regenerative cooling system,

$$q = h_{gc}(T_{aw} - T_{wg}), \tag{5.6}$$

$$q = \frac{k}{t}(T_{wg} - T_{wc}), \text{ and} \tag{5.7}$$

$$q = h_c(T_{wc} - T_{co}), \tag{5.8}$$

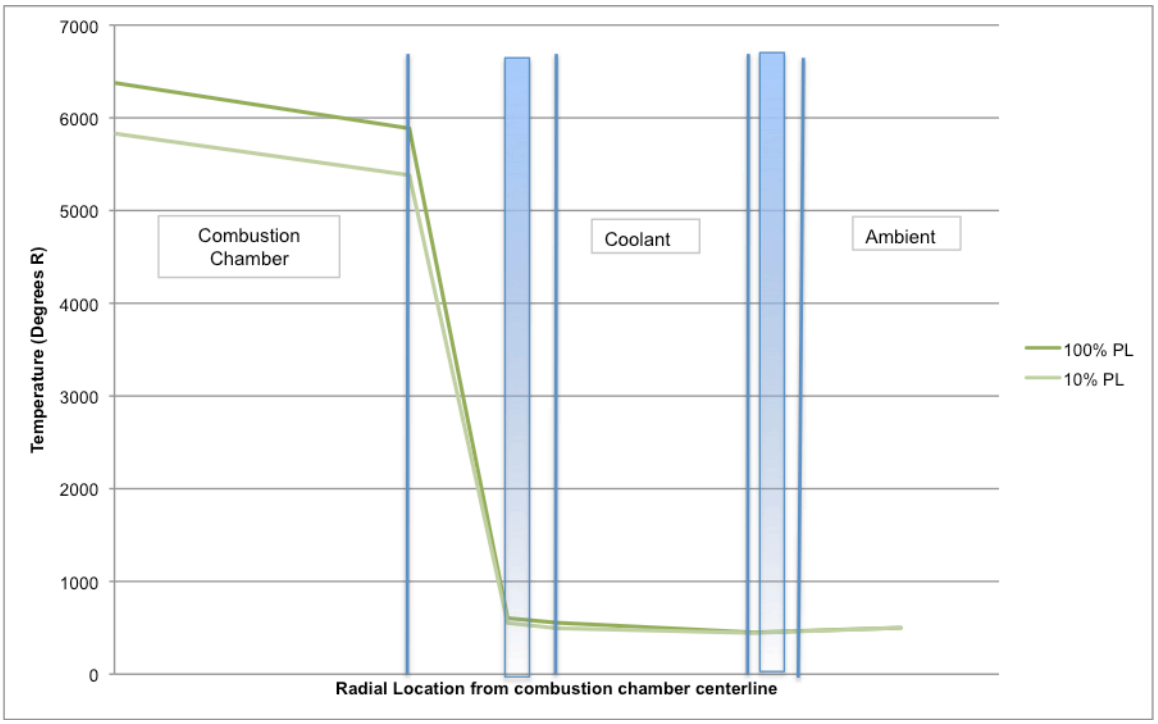

Figure 5.4: Results from Heat Transfer Through Regenerative Coolant Tubes

where q is the heat flux in Btu/in^2-s, h_{gc} is the gas-side thermal conductance in Btu/in^2-s-deg F, h_c is the coolant side heat transfer coefficient in Btu/in^2-s-deg F, k is the thermal conductivity of the chamber wall in Btu/in^2-s-deg F/in, t is the chamber wall thickness in inches, T_{aw} is the adiabatic wall temperature in degrees R, T_{wg} is the gas side wall temperature in degrees R, T_{wc} is the coolant side wall temperature in degrees R, and T_{co} is the coolant bulk temperature in degrees R.[5] Using these equations, overall heat transfer parameters are determined. The gas side heat transfer is calculated initially, followed by the coolant side for 100% power level. The coolant tubes are sized. The 10% power level calculations follow, using the same geometry that is set for the 100% power level.

Table 5.4: Results from Heat Transfer Analysis

		100% PL	10% PL	Units
Combustion Temperature	T_c	6377	5831	R
Adiabatic Wall Temperature	T_{aw}	5886	5382	R
Wall Temperature, Gas Side	T_{wg}	604	552	R
Wall Temperature, Coolant Side	T_{wc}	555	495	R
Adiabatic Wall Temperature, Coolant	T_{co}	450	444	R
Ambient Temperature	T_{amb}	500	500	R
Coolant Passage Inlet Temperature	T_{co_inlet}	180	180	R
Total Temp rise through cooling passages	ΔT_{co}	270	264	R
Total pressure drop through cooling passages	Δp_{co}	300	150	psia

A summary of the results from the heat transfer calculations at both 100% and 10% power is displayed in Figure 5.4 and Table 5.4.

5.6.1 Heat Transfer at 100% Power

In order to perform the gas-side heat transfer at 100% power, the heat flux is determined first. The gas-side thermal conductance is found using the combustion chamber gas properties and geometry. The adiabatic wall temperature T_{aw} is found by multiplying the chamber temperature by an effective recovery factor, which is assumed to be 0.93 in this case. The gas-side wall temperature is found using the equation,

$$T_{wg} = T_c - \left(\frac{2/3h_g}{2/3h_g + t/k} \right)(T_c - T_{ow}) \quad (5.9)$$

,

where the radiation is assumed to be 1/3 of the total heat flux, and T_c is the chamber temperature in degrees R, and T_{ow} is the outside wall, ambient temperature in degrees R. Equation (5.9) is derived from several equations that are found in Reference 5. Since h_{gc}, T_{aw}, and T_{wg} have been found, the heat flux q can be calculated using Equation (5.6).

Next, the wall coolant-side temperature is found. Since q is now known, the thermal conductivity of the chamber wall and the wall thickness is used with the gas-side wall temperature in order to find the T_{wc}, per Equation (5.7).

The next parameter to find is the coolant-side heat transfer coefficient. In this case, the coolant temperature that is desired, T_{co} is known, based on what temperature and pressure of propellant is needed at the fuel and oxidizer turbines in order for the turbines to generate enough horsepower to drive the pumps. Using Equation (5.8), h_c can be determined from q, T_{aw}, and T_{co}. In order to physically achieve the desired coolant-side heat transfer coefficient, several variables can be adjusted, such as the coolant tube hydraulic diameter and the number of tubes used. Since the geometry of the throat, chamber, and nozzle are set, and this heat transfer analysis is focused on the throat area, the hydraulic diameter and number of tubes are dependent on one another. It is also important to evaluate the fluid velocity through the coolant tubes and the Mach number of fluid through the coolant tubes at all power levels. The coolant tube hydraulic diameter is chosen to be 0.09 inches, and the number of tubes is determined to be 108, in order to fit around the 3.5 inch throat diameter. The pressure drop through the coolant tubes is assumed to be 300 psia, based on experience with regenerative cooled engines, and the coolant velocity is calculated from the equation

$$\Delta p = f \frac{L}{d} \frac{\rho V_{co}^2}{2g}, \tag{5.10}$$

where Δp is the pressure drop through the coolant tubes in psia, L is the length of travel through the coolant tubes in inches, d is the hydraulic diameter in inches, ρ is the density of methane under the coolant temperature and pressure in lb/in^3, g is the gravitational constant in in/s^2, and f is the friction loss factor, which is assumed to be 1.5 in this case.

Once the pressures, temperatures, and fluid velocity through the coolant tubes are calculated, the Mach number is determined to be 0.71 at 100% power. This Mach number makes sense since it indicates the flow is subsonic.

5.6.2 Heat Transfer at 10% Power

Now that the heat transfer for the 100% power level is calculated, the 10% power level is evaluated. As mentioned previously, the tube geometry is set from the 100% power level, so now the performance at 10% power is determined based on the 10% power methane flow rates and chamber pressure.

The gas side heat transfer is determined in the same manner that the 100% power gas side heat transfer is calculated using Equation (5.6). This includes determining the value for q, based on the combustion gas properties at 10% power and the set tube geometry.

For the coolant side heat transfer, T_{wg} is initially calculated using Equation (5.7). In order to be able to use Equation (5.8) to solve for the resulting T_{co}, the heat transfer coefficient h_c is needed. In order to find h_c at the 10% power level, the equation

$$q = \frac{.029 c_p \mu^{.2}}{\mathrm{Pr}^{2/3}} \frac{G^{.8}}{d^{.2}} \frac{T_{co}^{.55}}{T_{wc}^{.55}} (T_{wc} - T_{co}) \tag{5.11}$$

is used. Since all parameters except for T_{co} are known, Equation (5.11) can be solved for T_{co}.

Once the coolant temperature is known, it is necessary to find an appropriate coolant pressure that will give the methane gas the right properties in order to keep the Mach number in check. The primary driver in the Mach number is coolant speed and density. A pressure of 1000 psia is chosen. This pressure is iterated upon a bit in order to achieve the right pump and turbine performance, based on the gas properties at different pressures

using the coolant temperature that results from the combustion characteristics, engine geometry, and 10% power flowrates.

One point to note is that typically the coolant temperature rise through the coolant tubes is greater for lower power levels due to the increased stay time in the coolant tubes. In this case, at 10% power, the velocity of the gas is still fairly high, and there is a decrease in the heat flux through the coolant tubes due to the lower combustion chamber temperature. Thus, the added stay time does not overcome the lower heat flux as compared to 100% power, so the temperature rise at 10% power does not overcome the temperature rise at primary power level.

It is recommended that the regenerative cooling be evaluated in greater depth for this engine since this is an area that is critical to the engine's operation. This study provides for some rough estimates; however, there are many factors that can have a significant influence on the coolant properties that are not accounted for in this analysis, such as varying coolant properties and varying coolant tube geometry.

5.6.3 Additional Considerations for Regenerative Cooling

One issue that is worth mentioning within the coolant section is that when actual in-space ambient temperatures of 180 R are used on the external surface of the coolant tubes, the coolant stays too cold and it cannot pick up the heat required to drive the turbopumps. Thus, insulation is required on the exterior of the engine coolant tubes in order for the engine to operate in space. If an in-space ambient temperature of 180 R is used for the 100% power level, the T_{wg} is reduced to 289 R, which is insufficient to drive the fuel and oxidizer turbines. If the temperature on the outside of the coolant tubes is 500 R

(40 degrees F), the T_{wg} is 603 R at 100% power, which allows for adequate heat transfer into the coolant to drive the turbines. Ideally, the temperature on the outside of the coolant tubes should stay around 500 degrees R, which requires insulation to be added to the engine design.

Based on RP-1 propellant data, an estimate is made on the thermal resistance on the interior of the coolant tubes due to carbon deposits. The carbon deposits play a role in calculating the heat transfer coefficient on the gas wall side of the heat transfer analysis. The gas side heat transfer coefficient, h_g is calculated using standard means, excluding the thermal resistance due to the carbon deposits. However, when calculating the overall heat flux, q, the overall gas side thermal conductance, h_{gc} is used; h_{gc} takes into account the thermal resistance from the carbon deposits on the chamber walls. The equation for h_{gc} is

$$h_{gc} = \frac{1}{\frac{1}{h_g} + R_d}, \tag{5.12}$$

where R_d can range from 1100-2000 in^2-s-deg R/Btu. This is one item to note when using methane or any hydrocarbon propellant. This value can vary at different throttling levels, however, more data is needed from engine testing to adequately characterize this affect.

Validation of the results in this section is quite difficult without actual test data. It is difficult to compare the calculations to those in existing engines since there are so many factors that go into the calculations, such as material properties and contour of the chamber coolant tubes. Since the calculations used in this model are based on the calculations described in Reference 4, the results from this power balance model are compared to results for heat transfer examples that are worked in the textbook.[5] When using the same input parameters that are in the example problems, the same results are

achieved. This means that the equations and the logic used to develop the Mars lander power balance model are accurate.

5.6.4 Sensitivity Study on Heat Transfer

This section evaluates the effect of varied heat flux, driving a difference in adiabatic wall temperature on the hot gas side, and a difference in the coolant temperature on the interior of the regenerative coolant tubes. The engine is quite sensitive to heat flux, however it is believed that the tube wall thickness and material can be adjusted in order to achieved the desired heat flux to keep the chamber wall cool and to provide heat energy to the fuel so that it can drive the turbines at the desired speed.

The temperature profiles are evaluated as a function of heat flux, q (Btu/in^2-s). Since the material X-750 is chosen for the chamber wall, the temperature must stay below the yield temperature of 1460 degrees R. In evaluating this graph, which holds a constant 0.015 inch wall thickness, it is determined that the heat flux must stay above 1.15 Btu/in^2-s. Also, in order to keep the coolant temperature high enough to drive the turbines, the heat flux must stay below 1.35 Btu/in^2-s. This defines the useful heat flux range of 1.15 to 1.35 Btu/in^2-s at 100% power for this engine. A similar sensitivity study can be performed at 10% power. The results at 100% power are shown in Figure 5.5.

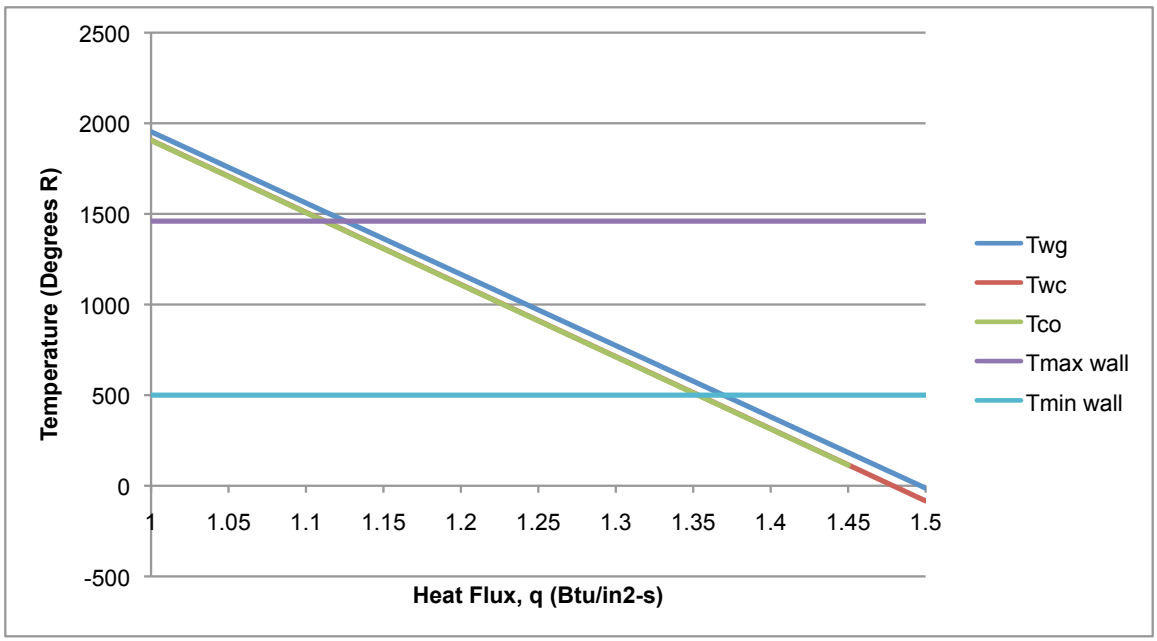

Figure 5.5: Sensitivity on Heat Flux at 100% Power

5.7 Turbine Design

The turbine design for this activity is performed at a fairly high level. In summary, the power requirement for the turbines can be determined from the power required to drive the pumps. In order to match the turbine power delivered to the pump power required, it is necessary to direct a portion of the fuel flow directly into the chamber using the thrust control valve and the oxidizer control valve. Bypassing the fuel turbine and the oxidizer turbine allow for fine control of the turbine drive power. The turbine efficiencies at 100% and at 10% power are determined based on experience with similar engines such as the RL-10 and J-2X, and the power is calculated using the equation

$$P = \dot{m}\eta_T c_p T_{in}\left(1 - \frac{p_{exit}}{p_{in}}\right)^{\frac{\gamma-1}{\gamma}}, \qquad (5.13)$$

where P is the turbine power in Btu/s, m is the mass flow rate in lbm/s, η_T is the turbine efficiency, c_p is the specific heat for methane at the turbine drive temperature and pressure in Btu/lb-deg F, T_{in} is the turbine inlet temperature in degrees F, p_{exit} is the turbine exit pressure, p_{in} is the turbine inlet pressure, and γ is the ratio of specific heats for methane at the turbine temperature and pressure.

The efficiency and pressure ratio are iterated upon in order to find a balance for power delivered by the turbine that matches the power required of the pumps, and to provide the oxidizer pump with inlet conditions that are slightly lower than the exit conditions of the turbine, to account for pressure and temperature losses in the ducting. The fuel turbine inlet temperature and pressure is determined from the regenerative coolant tube exit temperature and pressure.

As can be seen in the results of this assessment, the turbine power has the potential to significantly exceed the requirements of the turbopumps for both the fuel and oxidizer, at both 100% and 10% power. Thus, a portion of the flow is redirected by the thrust control valve directly to the injector faceplate, while the rest of the flow is sent through the turbine circuit. This redirected flow is used for cooling other engine components, such as valves and turbomachinery.

The fuel turbine carries a pressure ratio ($p_{discharge}/p_{inlet}$) of 0.9 at 100% power, and 0.698 at 10% power. At 100% power, 36.9% of the fuel flow is directed to the injector and other components that require cooling, while 63.1% of the flow is directed through the fuel turbine. This provides for a power of 170 Hp, which matches the power requirement of the fuel pump. At 10% power, 55% of the fuel flow is directed to the injector and other

components that require cooling, while 45% of the fuel is directed through the fuel turbine. This provides for a power of 25 Hp, which again matches the power required of the fuel pump at this power level.

Next in series is the oxidizer turbine. The oxidizer turbine operates at lower pressures and temperatures than the fuel turbine, due to lower power requirements for the oxidizer pump. The oxidizer turbine operates with a pressure ratio of 0.67 at 100% power and 0.20 at 10% power. At 100% power, 47% of the fuel flow from the fuel turbine exit is directed to the injector. This leaves 16.1% of the total engine fuel flow to power the oxidizer turbine. This provides for a power of 58.8 Hp, which matches the power requirement of the fuel pump. At 10% power, 33% of the fuel flow from the fuel turbine is directed to the injector. This leaves a mere 1.95% of the total engine fuel flow to power the oxidizer pump. This provides for a power of 2.7 Hp, which again matches the power required of the oxidizer pump at this power level.

In order to adequately determine the power delivered by the turbine at throttled power levels, testing is required, along with detailed turbine blade design in order to ensure stall does not occur during 10% power operation, along with the other issues outlined in Section 3.3.

Turbomachinery for throttling engines is designed for full thrust. When operating off the rated power level, special considerations need to be made for cavitation, rotordynamics, structural dynamics, bearings and fuel leakage flows, stall and velocity triangles, and surge. The detailed design of turbomachinery requires a large team of experienced engineers and the right development codes. This study is intended to outline

the issues that may arise due to throttling, and to provide a preliminary performance assessment of this hardware.

Validation of the turbine performance is similar to validation of the pump performance. The J-2X turbine drive characteristics, inputs, outputs and efficiencies from the J-2X turbines are used in the model. Setting the percent of flow through the turbine to 100%, the Mars lander model provides similar results for turbine power generated that are generated in the governing J-2X power balance model. This provides for confidence that the equations used here are used correctly.

5.8 Assessment of Success Criteria

As displayed in the preceding sections, a new Mars lander throttling engine has been developed with a thrust range of 1,500 to 15,000 lbf. The engine demonstrates an expander cycle using LOX and methane as propellants. The component performance parameters that are achieved in the model are within American flight and ground test capabilities.

The success criteria for the design study have been met:

- The power balance model that is developed as a part of this study closes for both 100% and 10% power levels, using reasonable assumptions based on historical liquid rocket engine experience, and using basic design equations.
- The power balance model demonstrates that a ratio of $\Delta p/p_c$ of 20% can be achieved at both 100% and 10% power levels using reasonable engine feed pressures and temperatures. The feed pressures are 45 psia for both the fuel and the oxidizer, and the feed temperatures are cryogenic for both propellants. This is within the American

experience base with propellants, and is considered to be acceptable for propellant feed conditions.

- Reasonable pump performance parameters are achieved, and the pump calculations are validated by comparison to J-2X oxidizer pump performance predictions.
- Adequate cooling from the fuel in the regenerative cooling channels is achieved at both power levels. The heat transfer is adequate to keep the selected chamber material below its maximum allowed operating temperature. The selected wall material is Alloy X-750, and the temperature is required to stay below 1460 degrees R. This is achieved, as the wall temperature does not exceed 604 degrees R.
- An adequate temperature rise in the coolant fuel is achieved in order to successfully drive the fuel and oxidizer turbines to power the fuel and oxidizer pumps. There is excess energy available from the fuel that is not needed to drive the turbines at both power levels. This excess fuel is routed throughout the engine and is used for cooling components such as the turbopump and valve internal components.

Although more thorough model validation is required before there is a high degree of confidence in the results, based on independent component validation, it is believed that power balance model generated in this study does indeed provide fairly reliable results. J-2X and RL-10 CECE data is used to help validate individual component calculations.

CHAPTER SIX

CONCLUSIONS AND FUTURE WORK

This study on liquid rocket engine throttling demonstrates that it is feasible to design a Mars lander engine that uses LOX and methane propellants and can throttle from 15,000 to 1,500 lbf thrust. After performing a literature search and laying out the systems considerations for a throttling engine, a power balance model is developed for the Mars lander engine. A top-level assessment is made of the performance parameters for the turbopumps, drive turbines, and the regenerative coolant chamber. A pintle injector is selected due to its demonstrated ease of use in a throttling engine, with is ability to vary the propellant flow area for injection into the combustion chamber.

While this is a top-level study, further work is required in order to validate the model that is developed during this study. It would take a sizeable team of people to dive into the detailed design work to thoroughly design the pumps, turbines, valves, and nozzle contour. Engine testing will provide for the true test of throttleability, since there are many nuances that are discovered during a test program that cannot be predicted using analytical models.

An attempt is made in this study to perform preliminary validation of the calculations used for each component by using J-2X and RL-10 CECE data in the model to see if the same results are obtained. There is a high degree of confidence in the ISP CEA Model

results that are used for the preliminary thrust chamber parameters, since ISP CEA Model results have been checked against test data for SSME, CECE, RD-180, RL-10, and J-2X. The individual component calculations are also reliable since results can be achieved that are very close to results achieved using the governing J-2X and RL-10 power balance models when the component input and output parameters for J-2X and RL-10 are used.

Liquid rocket engine throttling has been required on past space missions, and it will be required on future missions, whether the destination is the moon, Mars, or a near-Earth object. Although most of the current literature on throttling is devoted to the injector, throttling is a system issues that touches every component on the engine and the feed system. It is critical for the future of the U.S. space program to continue to study methods for throttling to better understand liquid rocket engine functionality and sensitivities, as throttling components can also be used in advanced propulsion systems such as nuclear-thermal in addition to liquid rocket engine systems.

APPENDICES

APPENDIX A

POWER BALANCE RESULTS

This section documents the results that are obtained from the power balance model that is developed for the Mars lander engine in this study. Table A.1 shows the LOX circuit, and Table A.2 shows the Fuel circuit. Figure A.1 shows the engine schematic with node points that are referenced in the tables.

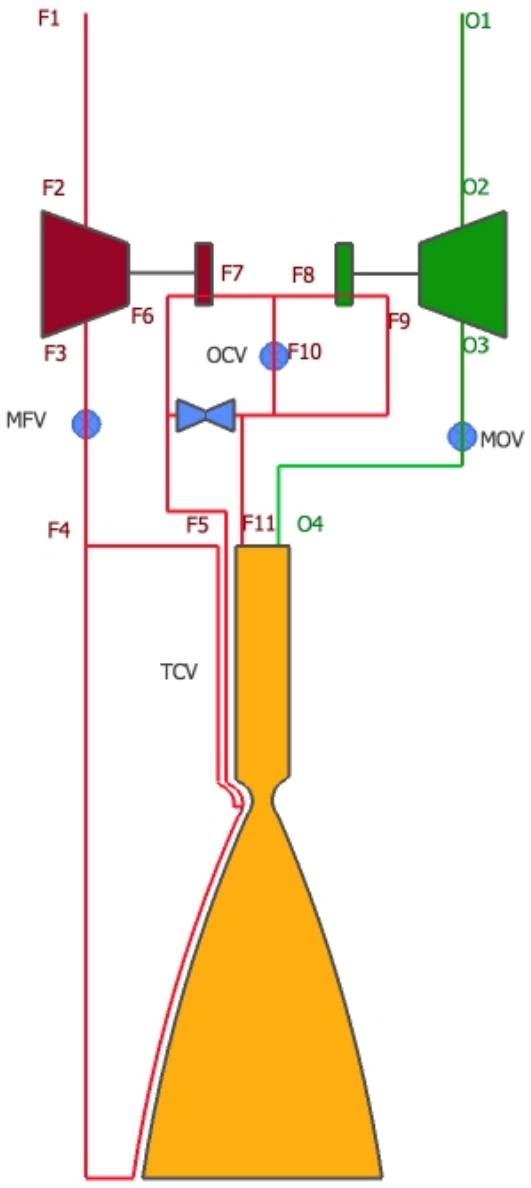

Figure A.1: Mars Lander Engine Flow Schematic

Table A.1: Oxidizer Flow Circuit

Oxidizer		100% PL	10% PL
O1	**Oxidizer Feed**		
	p_fuel_inlet (psia)	45	45
	T_fuel_inlet (R)	163	163
O2	**Ox Pump Inlet**		
	p_OP_inlet (psia)	43.65	43.65
	T_OP_inlet (R)	163	163
O3	**Ox Pump Exit**		
	p_OP_exit (psia)	1008	101
	T_OP_exit (R)	171	164
	N_OP (rpm)	36968	8250
	HP_OP_required (HP)	58.87	2.67
	η_OP	60%	40%
	ΔH_OP (ft)	1945	174
O4	**Ox Injector Inlet**		
	p_Ox_injector (psia)	960	96
	T_Ox_injector (R)	170	170

Table A.2: Fuel Flow Circuit

Fuel		100% PL	10% PL
F1	**Fuel Feed**		
	p_fuel_inlet (psia)	45	45
	T_fuel_inlet (R)	172	172
F2	**Fuel Pump Inlet**		
	p_FP_inlet (psia)	44.1	44.1
	T_FP_inlet (R)	173	173
F3	**Fuel Pump Exit**		
	p_FP_exit (psia)	2000	1155
	T_FP_exit (R)	181	181
	N_FP (rpm)	53607	36000
	HP_FP_required (HP)	170.12	24.94
	η_FP	64%	43%
	ΔH_FP (ft) Total, 2 stages	5987	5740
F4	**Cooling Channel Inlet**		
	p_cool_inlet (psia)	1980	1150
	T_cool_inlet (R)	180	180
F5	**Cooling Channel Exit**		
	p_cool_exit (psia)	1680	1000
	T_cool_exit (R)	450	444
F6	**Fuel Turbine Inlet**		
	Flow Bypassed using TCV	36.9%	55.0%
	p_FT_inlet (psia)	1660	995
	T_FT_inlet (R)	445	439
F7	**Fuel Turbine Exit**		
	p_FT_exit (psia)	245	339
	T_FT_exit (R)	1660	995
	HP_FT_provided (HP)	170.18	25.11
	η_FT	70%	60%
F8	**Ox Turbine Inlet**		
	Flow Bypassed using OTBV	47.00%	43.05%
	p_OT_Inlet (psia)	1490	500
	T_OT_inlet (R)	243	322
F9	**Ox Turbine Exit**		
	p_OT_exit (psia)	1000	100
	T_OT_exit (R)	189	189
	HP_OT_provided (HP)	59	3
	η_OT	70%	60%
F11	**Injector Fuel Inlet**		
	p_fuel_inj (psia)	960	96
	T_fuel_inj (R)	180	180

APPENDIX B

TURBOPUMP MAPS

This section provides an example of how the generic pump map is used to calculate pump performance at the throttled 10% thrust level. Table B.1 is the generic pump map that is used in these calculations.

Table B.1: Generic Pump Maps

Generic Pump Maps			
PHIN	PSIN	PHIN	TAUN
-0.400	1.310	-0.400	0.400
-0.300	1.300	-0.300	0.380
-0.200	1.290	-0.200	0.400
0.000	1.260	0.000	0.480
0.500	1.210	0.500	0.800
0.700	1.150	0.700	0.900
0.800	1.110	0.800	0.935
0.900	1.080	0.900	0.975
1.000	1.000	1.000	1.000
1.100	0.930	1.100	1.020
1.200	0.840	1.200	1.030
1.300	0.750	1.300	1.035
1.500	0.480	1.500	1.010
2.000	-0.250	2.000	0.850
2.500	-1.060	2.500	0.530
		3.000	0.000

Table B.2: Calculated Oxidizer Pump Performance Parameters

Parameter	Variable	Units	100% PL
Pump pressure rise required	Δp	psi	964.35
LOX fluid density	ρ	lbm/in^3	0.041308
Pump speed	N	rpm	36967.72
Pump speed	N	rad/s	3871.251
Pump head rise	ΔH	ft	1945.453
Pump specific speed	S	Unitless	1000
Volumetric flowrate	Q	gpm	62.7893
Oxidizer Mass flowrate	$\dot{m}$	lbm/s	32.95287

The example problem is for the LOX turbopump. Initially, the 100% performance parameters are determined. At 100% thrust, both ϕ_N and ψ_N are equal to one, since the coefficients are normalized to the 100% power level.

Initially, the speed is determined using Equation (5.3)

$$N = \frac{\Delta H S^{.75}}{Q} \quad ,$$

where ΔH is the pump head rise in ft, S is the pump specific speed, and Q is the volumetric flowrate in gpm. The values used for ΔH, S, and Q are shown in Table B.2. The speed calculated using this equation is in units of revolutions per minute, or rpm. When the speed is used in the head and flow coefficient calculations, the units radians per second are used, so the pump speed needs to be converted to these units by multiplying the speed in rpm by $\pi/30$.

Now that the pump speed is known, Equation (5.1)

$$\psi_N = \frac{\Delta p}{\rho N^2} \times \frac{1}{\psi_D}$$

is used to calculate the design head coefficient. The normalized head coefficient is set equal to 1, and the design head coefficient is solved for,

$$\psi_D = \frac{\Delta p}{\rho N^2 \psi_N} = \frac{(964.35\,psi)}{(.041308\,\frac{lbm}{in^3})(3871.251\,\frac{rad}{s})^2(1)} = 0.00156.$$

Next, Equation (5.2)

$$\phi_N = \frac{\dot{m}}{\rho N} \times \frac{1}{\phi_D}$$

is used to calculate the design flow coefficient. The normalized flow coefficient is set equal to 1, and the design flow coefficient is found to be

$$\phi_D = \frac{\dot{m}}{\rho N \phi_N} = \frac{(32.95287\,\frac{lbm}{s})}{(.041308\,\frac{lbm}{in^3})(3871.251\,\frac{rad}{s})(1)} = 0.20607.$$

At this point, the design and normalized head and flow coefficients for the oxidizer pump are known at 100% power. Now, these coefficients are used to calculate the pump performance at the 10% throttled power level. The design coefficients remain constant, and at 10% power the mass flow rate, oxidizer density, and required pressure rise is known. The pump maps are used in order to find the pump speed at the throttled performance level that is required to provide the necessary pressure rise. Equation (5.3) is no longer used to calculate the pump speed.

In order to find the right combination of pump speed and head coefficient, iteration is required. First, a pump speed is guessed. The normalized flow coefficient is found using Equation (5.2). The normalized flow coefficient is used with the relationships in Table B.1 to find the normalized head coefficient. The normalized head coefficient is then used in Equation (5.1) along with the guessed pump speed to find the Δp. Manual iteration on pump speed is performed until the desired value for Δp is achieved. The target Δp at 10% power for the oxidizer pump is 57.15 psi.

For this problem, an initial speed of 20,000 rpm (2,094 rad/s) is chosen. Rearranging Equation (5.2), the normalized flow coefficient is determined

$$\phi_N = \frac{\dot{m}}{\rho N \phi_D} = \frac{3.375 \frac{lbm}{s}}{(0.0413 \frac{lbm}{in^3})(2094 \frac{rad}{s})(0.20607)} = 0.189.$$

Next, using the pump map Table B.1, a relationship is determined to find the normalized head coefficient,

$$\frac{0.500 - 0.189}{1.210 - \psi_N} = \frac{0.500 - 0.000}{1.210 - 1.260}, \text{ therefore } \psi_N = 1.24106.$$

Now that ψ_N is known, Δp is calculated using Equation (5.1)

$$\Delta p = \rho N^2 \psi_D \psi_N = (.0413 \frac{lbm}{in^3})(2094 \frac{rad}{s})^2 (0.001556)(1.24106) = 3{,}497.08\, psi.$$

This value of 3,497.08 psi is too high for the throttled performance level. Thus, a lower speed is guessed and the same process is repeated until a value of approximately 57.15 psia for Δp is found.

The final guess for speed after a series of iteration is N = 8250 rpm (863.94 rad/s).

$$\phi_N = \frac{\dot{m}}{\rho N \phi_D} = \frac{3.375 \frac{lbm}{s}}{(0.0413 \frac{lbm}{in^3})(863.94 \frac{rad}{s})(0.20607)} = .459$$

$$\frac{0.500 - 0.459}{1.210 - \psi_N} = \frac{0.500 - 0.000}{1.210 - 1.260}, \text{ therefore } \psi_N = 1.214$$

$$\Delta p = \rho N^2 \psi_D \psi_N = (.0413 \frac{lbm}{in^3})(863.94 \frac{rad}{s})^2 (0.001556)(1.214) = 58\, psi.$$

The iteration is stopped at this point since 58 psia is sufficiently close to the desired value for Δp.

In summary, Table B.3 displays the results for the oxidizer pump performance using generic pump maps.

Table B.3: Oxidizer Performance from using Generic Pump Maps

Parameter	100% PL	10% PL
ψ_N	1	1.214
ϕ_N	1	0.459
ψ_D	0.001558	0.001558
ϕ_D	0.206067	0.206067
Δp (psi)	964	58
N (rpm)	36968	8250

REFERENCES

[1] Griffin, M. D. and French, J. R., "Launch Vehicle Selection," *Space Vehicle Design*, 2nd Edition, AIAA Education Series, Virginia, 2004.

[2] Welton, D.E., Bensky, M.S. and Hiland, J., "Variable Thrust Liquid Propellant Rocket Engines," AIAA Paper 1963-0268, June 1963.

[3] Casiano, M. J., Hulka, J. R. and Yang, V., "Liquid-Propellant Rocket Engine Throttling: A Comprehensive Review," AIAA Paper 2009-5135, August 2009.

[4] Giuliano, V. J., Leonard, T. G. and Kim, T. S., "Development Status of the CECE Cryogenic Deep Throttling Demonstrator Engine," Space Propulsion 2008, 2nd International Symposium on Propulsion for Space Transportation, 2008.

[5] Huzel, D. K. and Huang, D. H., *Modern Engineering for Design of Liquid-Propellant Rocket Engines,* Progress in Astronautics and Aeronautics Volume 147, AIAA, Washington D.C., 1992.

[6] Dressler, G.A., "Summary of Deep Throttling Rocket Engines with Emphasis on Apollo LMDE," AIAA Paper 2006-5220, July 2006.

[7] Aerojet, "Aerojet Awarded NASA Contract for Unique LOX-Hydrogen Deep Throttling Injector Development," http://spacefellowship.com/news/art15675/aerojet-awarded-nasa-contract-for-unique-lox-hydrogen-injector.html [retrieved 1 May, 2010].

[8] Dressler, G.A. and Bauer, J.M., "TRW Pintle Engine Heritage and Performance Characteristics," AIAA Paper 2000-3871, July 2000.

[9] Elverum, Jr., G., Staudhammer, P., Miller, J., Hoffman, A. and Rockow, R., "The Descent Engine for the Lunar Module," AIAA Paper 67-521, July 1967.

[10] Casiano, M. J., Interview on Throttling Techniques, 9 April 2010.

[11] Tanner, L. G., "Development and Characteristics of the Russian/American RD-180 Rocket Engine," *AIAA Liquid Propulsion Short Course*, Presented at the AIAA Liquid Propulsion Conference, Indiana, July 2002.

[12] Hardgrove, J.A. and Krieg, H., "High Performance Throttling and Pulsing Rocket Engine," AIAA Paper 1984-1254, June 1984.

[13] Werrell, K. P., "The Evolution of the Cruise Missile," Air University, Maxwell Air Force Base, AL, September 1985.

[14] Birkenstaedt, B. M., Hopkins, J., Kutter, B., Zegler, F. and Mosher, T., "Lunar Lander Configurations Incorporating Accessibility, Mobility, and Centaur Cryogenic Propulsion Experience," AIAA Paper 2006-7284, September 2006.

[15] "In-situ Exploration and Sample Return: Entry, Descent, and Landing," Mars Rover NASA Website, http://marsrover.nasa.gov/technology/is_entry_descent_landing.html [retrieved Feb 24, 2010].

[16] Betts, E. M. and Frederick, R. A., "A Comprehensive Systems Study of Liquid Rocket Engine Throttling Capabilities ," AIAA Paper 2010-6541, July 2010.

[17] Gilroy, R. and Sackheim, R., "The Lunar Module Descent Engine - A Historical Summary," AIAA Paper 89-2385, July 1989.

[18] Santiago, J. R., "Evolution of the RL10 Liquid Rocket Engine for a New Upperstage Application," AIAA Paper 96-3013, July 1996.

[19] Pugh, R. L., "The Many Facets of the RL-10 Liquid Rocket Engine…A Continuing Success Story," AIAA Paper 98-3680, July 1998.

[20] Limerick, C., "Component Design Concerns for Deep Throttling H_2/O_2 Rocket Engines," AIAA Paper 91-2209, June 1991.

[21] Wanhainen, J. P., Antl, R. J., Hannum, N. P. and Mansour, A. H., "Throttling Characteristics of a Hydrogen-Oxygen, Regeneratively Cooled, Pump-Fed Rocket Engine," NASA TM X-1043, December 1964.

[22] Stepanoff, A.J., "Centrifugal and Axial Flow Pumps Theory, Design, and Application," 2nd Edition, Krieger Publishing Company, Malabar, Florida, 1957.

[23] Brennen, C. E., "Hydrodynamics of Pumps," Concepts ETI, Inc. and Oxford University Press, Norwich, Vermont, 1994.

[24] Blair, J.C., Ryan, R.S. and Schutzenhofer, L.A., "Launch Vehicle Design Process: Characterization, Technical Integration, and Lessons Learned," NASA TP-2001-210992, Marshall Space Flight Center, May 2001.

[25] Marsh, M., Interview on Turbopump Design for Variable Thrust Applications, 18 March 2010.

[26] Brown, A.M., "Comprehensive Structural Dynamic Analysis of the SSME/AT Fuel Pump First-Stage Turbine Blade," NASA TM-1998-208594, Marshall Space Flight Center, Alabama, 1998.

[27] Alvarez, E., Interview on Turbopump Design for Variable Thrust Applications, 16 March 2010.

[28] Japikse, D. and Baines, N. C., "Stability and Range," *Introduction to Turbomachinery*, Concepts ETI, Inc and Oxford University Press, White River Junction, Vermont, 1997.

[29] Wong, G.S., Macgregor, C.A. and Hoshide, R.K., "Suppression of Cavitation and Nonstable Flow in Throttled Turbopumps," *Journal of Spacecraft and Rockets*, Vol. 2, No. 1, February 1965.

[30] Limerick, C. D. and Brown, J. R., "Expander Cycle Engine Applicability to Advanced Space Mission," JANNAF Paper, May 1989.

[31] Greitzer, E. M., "The Stability of Pumping Systems - The 1980 Freeman Scholar Lecture," *Journal of Fluids Engineering*, Vol. 103, June 1981.

[32] Harvey, D. W., "Throttling Venturi Valves for Liquid Rocket Engines," AIAA Paper 70-0703, June 1970.

[33] Fuller, P. N., "J-2S Nozzle Side-Load Study Final Report," NASA Contract NAS8-25156, August 1972.

[34] Sutton, G. P., *History of Liquid Propellant Rocket Engines*, AIAA, Reston, VA, 2006.

[35] Brown, A. M., Ruf, J. H., and McDaniels, D. M., "Recovering Aerodynamic Side Loads on Rocket Nozzles using Quasi-Static Strain-Gage Measurements," AIAA Paper 2009-2681, August 2009.

[36] Rachuk, V. S., Shostak, A. V., Dmitrenko, A. I., Goncharov, G. I., Hernandez, R., Starle, R. G. and Hulka, J., "Benchmark Testing of an Enhanced Operability LO2/LH2 RD-0120 Engine," AIAA Paper 96-2609, July 1996.

[37] Sutton, G. P. and Biblarz, O., *Rocket Propulsion Elements*, 7th Edition, John Wiley & Sons, Inc., New York, 2001.

[38] Humble, R. W., Henry, G. N. and Larson, W. J., *Space Propulsion Analysis and Design*, Space Technologies Series, McGraw Hill, New York, 1995.

[39] "A3.0 System Design Improvements," NASA Johnson Space Center Human Exploration website, http://ares.jsc.nasa.gov/HumanExplore/Exploration/EXLibrary/docs/MarsRef/addendum/A3.htm [retrieved March 4, 2011].